

Performance Evaluation of Reclaimed Asphalt Pavement in Hot Mix Asphalt Modified
with Organosilane

by

Phani Sasank Kaligotla

A Thesis Presented in Partial Fulfillment
of the Requirements for the Degree
Master of Science

Approved April 2018 by
Graduate Supervisory Committee:

Kamil Kaloush, Chair
Michael Mamlouk
Jeffrey Stempihar

ARIZONA STATE UNIVERSITY

May 2018

ABSTRACT

Use of Recycled Asphalt Pavement (RAP) in newly designed asphalt mixtures is becoming a common practice. Depending on the percentage of RAP, the stiffness of the hot mix asphalt (HMA) increases by incorporating RAP in mixes. In a climatic area such as the City of Phoenix, RAP properties are expected to be more oxidized and aged compared to other regions across the US. Therefore, there are concerns about the cracking behavior and long-term performance of asphalt mixes with high percentage of RAP. The use of Organosilane (OS) in this study was hypothesized to reduce the additional cracking potential and improve resistance to moisture damage of the asphalt mixtures when using RAP. OS has also the potential to improve the bond between the aggregate and asphalt binder. The use of OS also reduces the mixing and compaction temperatures required for asphalt mixtures, making it similar to a warm mix asphalt (WMA),

Six asphalt mixes were prepared with three RAP contents, 0%, 15% and 25%, with and without Organosilane. The mixing temperature was reduced by 10°C and the compaction temperature was reduced by 30°C. Mix designs were performed, and the volumetric properties were compared. The mixture laboratory performance was evaluated for all mixtures by conducting Dynamic Modulus, Flow Number and Tensile Strength Ratio tests.

The study findings showed that mixtures achieved better compaction at a reduced temperature of 30°C. Mixtures modified with Organosilane generally exhibited softer behavior at the extreme ends of lower and higher temperatures. The lower moduli are to reduce the potential for cracking. For the Flow Number test, the RAP mixtures with OS

passed the minimum required at all traffic levels. Tensile Strength Ratio results increased with the increase in RAP percentage, and further increase was observed when OS was used. The OS reduced the sticking nature of the binder to the molds and equipment, which reduced the efforts in cleaning them.

Finally, the future use of RAP by the City of Phoenix would positively contribute to their sustainability aspiration and initiatives. The use of Organosilane may even facilitate higher percentage of RAP usage; it definitely improves the moisture resistance of asphalt mixtures, especially when lower mixing and compaction temperatures are desired or used.

I would like to dedicate this work to my parents and family who have always advised and supported me in every step of my life.

ACKNOWLEDGMENTS

I would like to thank my advisor Dr. Kamil Kaloush for giving this opportunity to work with him. I thank him for his support and advice given to me throughout the project. I would also like to thank Drs. Mamlouk and Stempihar for their support and being on my committee. This work also started while Dr. Shane Underwood was at ASU and I would like to acknowledge his earlier support.

I would like to acknowledge all the graduate students at Arizona State University who helped me in operating the equipment and guided me when I have doubts. I would also thank Jeff Long, Lab Technician for helping me whenever I needed help.

I would like to thank Southwest Asphalt, El Mirage pit for providing the aggregate and processed Reclaimed Asphalt Pavement. I Would like to thank Western Refining, Phoenix, for providing the asphalt binder. Special thanks are also due for Stratis Giannakouros of the Global Sustainability Studies at ASU, and the City of Phoenix staff (Peter Rupal, Ryan Stevens, Robert Duvall, and others) for providing the opportunity to work on the City's RAP project.

Last but not least, I would like to thank Zydex industries, Vadodara, India, for providing the Organosilane product.

TABLE OF CONTENTS

	Page
LIST OF TABLES	viii
LIST OF ABBREVIATIONS.....	xii
LIST OF SYMBOLS	xiii
CHAPTER	
1 Introduction.....	1
1.1 Background.....	1
1.2 Objective	2
1.3 Scope.....	3
1.4 Organization of Report	3
2 Literature review	5
2.1 Recycled Asphalt Pavements	5
2.1.1 Studies on RAP mixes	5
2.1.2 Handling RAP in the Laboratory	8
2.2 Warm Mix Asphalt	10
2.3 Organosilane	11
3 Materials and Properties	16
3.1 Aggregate	16
3.2 Asphalt Binder	17

CHAPTER	Page
3.3 Recycled Asphalt Pavement	18
3.4 Organosilane	21
4 Experimental procedure	27
4.1 Mix design	27
4.1.1 Mixing	27
4.1.2 Theoretical Maximum Specific Gravity (G_{mm}).....	30
4.1.3 Bulk Specific Gravity of Compacted Hot Mix Asphalt (G_{mb}).....	31
4.1.4 Mix design calculations	31
4.2 Performance tests	33
4.2.1 Sample preparation	33
4.2.2 Dynamic Modulus.....	35
4.2.3 Flow Number	37
4.2.4 Tensile strength Ratio	40
5 Results and Analysis	44
5.1 Mix design	44
5.2 Dynamic modulus	47
5.2.1 Master curves generated using dynamic modulus results for all mixtures	48

CHAPTER	Page
5.2.2 Comparison of Modulus values of all mixtures at all frequencies for each temperature	51
5.3 Flow Number	55
5.4 Tensile strength Ratio	58
6 Summary, Conclusions and Recommendations.....	62
6.1 Summary	62
6.2 Conclusions.....	63
6.3 Recommendations for Future Work.....	65
REFERENCES	66
APPENDIX	
A Mix Design Calculations.....	69
B Dynamic Modulus Test Results	74
C Flow Number Results.....	82
D Tensile Strength Ratio Calculations.....	87

LIST OF TABLES

Table	Page
3.1 Properties of Combined Aggregate.....	16
3.2 Gradation for Dense Graded Mix with NMAS 19 mm (3/4")	17
3.3 Properties of PG 70-10 Asphalt Binder	17
3.4 Gradation Comparison of RAP and Extracted RAP Aggregate with City of Phoenix Limits (Phoenix, 2015)	19
3.5 Specific Gravity Values for Extracted RAP Aggregate.....	20
3.6 Dosage of OS Depending on The Type of Mixture.....	23
3.7 Dynamic Shear Rheometer Test Results for Organosilane Modified and Unmodified Binder.....	26
5.1 Volumetric Properties of 0% RAP Mix	44
5.2 Volumetric Properties of 15% RAP Mix	44
5.3 Volumetric Properties of 25% RAP Mix	45
5.4 Comparison of all The Volumetric Properties of RAP Mixes.....	46
5.5 Effect of OS on Air Voids of Mix	46
5.6 Parameters for Sigmoidal Equation of Dynamic Modulus Determined from Master Curve.....	48
5.7 Flow Number (FN) Values for all Six Mixes	55
5.8 Rut Depth (in) Calculated for 3 in Thick Layer for Different ESALs.....	57
5.9 Flow Number Values at Different Stress Levels Calculated Using Flow Number Prediction Equation.....	58

Table	Page
5.10 Minimum Average Flow Number Values for Different Traffic Levels (AASHTO-TP79-15, 2016)	58
5.11 Tensile Strength Ratio Results for Control Mix	59
5.12 Tensile Strength Ratio Test Results for 0% RAP Mix with OS	59
5.13 Tensile Strength Ratio Test Results of 15% RAP Mix.....	59
5.14 Tensile Strength Ratio Test Results for 15% RAP Mix with OS	59
5.15 Tensile Strength Ratio Test Results for 25% RAP Mix	60
5.16 Tensile Strength Ratio Test Results 25% RAP Mix with OS.....	60
5.17 Comparison of TSR Values of all Mixes.....	61

LIST OF FIGURES

Figure	Page
2.1 Moisture Content Changes for RAP Dried in an Oven (Randy West, 2013)	9
2.2 Organosilane Alkylalkoxy Compound (Ajay Ranka, 2014).....	11
2.3 All Possible Reactions Between Substrate and Organosilane (Ajay Ranka, 2014)....	12
2.4 Silane Reaction on Aggregate Surface (Ranka, 2014).....	13
3.1 Processed RAP Material at Southwest Asphalt, El Mirage Plant	18
3.2 RAP and Extracted Aggregate Gradation.	19
3.3 Experiments of Heating RAP Before Mixing.....	21
3.4 Cleaner Equipment Due to Non-sticky Nature of OS Modified Binder.....	22
3.5 High Shear Mixer.....	23
3.6 Adding OS to Asphalt at 150°C.....	24
3.7 Viscosity of Organosilane (Zydexmodified and unmodified binders at different temperatures	25
4.1 Heating aggregate at mixing temperature	28
4.2 Mixing of aggregate and binder	29
4.3 Spreading the HMA flat on pan for short term aging	29
4.4 Gyratory compactor	30
4.5 Specimen cored and cut from compacted size to required size.	34
4.6 Schematic of gauge points for dynamic modulus and flow number samples (AASHTO-TP79-15, 2016)	35
4.7 Specimen for dynamic modulus testing.....	36
4.8 Flow number testing for sample	38

Figure	Page
4.9 Flow number sample after completion of test.....	39
4.10 Indirect tensile strength test	42
5.1 Comparison of Compaction curves with and without OS	47
5.2 Master curve comparison of all RAP mixes	48
5.3 Master curve comparison between 0% RAP mixes with and without OS.....	49
5.4 Master curve comparison for 15% RAP mixes with and without OS	50
5.5 Master curve comparison for 25% RAP mixes with and without OS	50
5.6 Master curve comparison for all the mixes.....	51
5.7 Modulus comparison of all mixtures at all frequencies at -10C	52
5.8 Modulus comparison of all mixtures at all frequencies at 4.4 C	53
5.9 Modulus comparison of all mixtures at all frequencies at 21.1C	53
5.10 Modulus comparison for all mixtures at all frequencies at 37.8C	54
5.11 Modulus comparison for all mixtures at all frequencies at 54.4 C	54
5.12 Comparison of flow number values for all six mixes	56
5.13 Comparison plot for TSR values of all mixes.....	60

LIST OF ABBREVIATIONS

1. AASHTO- American Association of State Highway and Transportation Officials
2. AMPT- Asphalt Mixture Performance Tester
3. DSR- Dynamic Shear Rheometer
4. FHWA - Federal Highway Administration
5. HMA- Hot Mix Asphalt
6. LTPP - Long-Term Pavement Performance
7. MEPDG - Mechanistic-Empirical Pavement Design Guide
8. NCHRP- National Cooperative Highway Research Program
9. NMAS - Nominal Maximum Aggregate Size
10. PAV - Pressure Aging Vessel
11. PG - Performance Grade
12. RAP - Reclaimed/Recycled Asphalt Pavement-
13. RTFO- Rolling-Thin Film oven
14. RV- Rotational Viscosity
15. SBS - Styrene-Butadiene-Styrene
16. TSR- Tensile Strength Ratio
17. VFA - Voids Filled with Asphalt
18. VMA - Voids in Mineral Aggregate
19. WMA- Warm Mix Asphalt
20. ZT- Zycotherm

LIST OF SYMBOLS

1. G_{mm} - Theoretical Maximum Specific Gravity
2. G_{mb} - Bulk Specific Gravity
3. N_{ini} - Gyration for initial density
4. N_{dsg} - Gyration for design density
5. N_{max} - Gyration for maximum density
6. ρ - Density
7. d - Diameter
8. t - Thickness
9. h - Height

Chapter 1 Introduction

1.1 Background

Over 90 percent of United States highways and roads are constructed by using Hot Mix Asphalt (HMA) (Copeland, 2011). HMA mainly consists of about 95% aggregate and the remaining is the binder (asphalt). Both of these materials are non-renewable resources and their quantities are diminishing. According to FHWA recycled material policy “The same materials used to build the original highway system can be re-used to repair, reconstruct, and maintain them. Where appropriate, recycling of aggregates and other highway construction materials makes sound economic, environmental, and engineering sense” (Copeland, 2011). Thus, the HMA producers started using Recycled Asphalt Pavement (RAP) in their mixtures as the supply of aggregates and binder has been limited.

In the present day, Reclaimed Asphalt Pavement is a valuable component of Hot Mix Asphalt. It is the millings of old pavements which still has the old oxidized binder. Use of RAP became popular in 1970 when the oil prices raised up because of Arab oil embargo (West, 2010). As RAP reduces the use of virgin aggregate and binder, agencies have replaced some percentage of virgin material with RAP. Usage of RAP has both environmental benefits and economic savings. RAP also reduces the debris from asphalt millings that are dumped in landfills. The usage of RAP by the department of transportations has become a common practice.

Another problem faced by asphalt pavements is related to the presence of moisture. Many of the asphalt pavements failures are attributed to distress caused by

moisture (Ajay Ranka, 2014). The moisture causes the early loss of strength and durability of pavements. Moisture enters the pavement through air voids, weakens the asphalt-aggregate structure, and reduces the cohesive strength causing failure of the pavement layer. The cohesive and adhesive failures in asphalt pavements occur due to pore pressure, displacement, detachment, and interfacial tension. Displacement occurs because of stripping of asphalt from aggregate majorly caused due to the uneven coating of asphalt, traffic and freeze-thaw cycles causing stress in pavement resulting several types of distresses (Zaniewski J, 2006).

When the penetrated water interacts with the aggregate surface, it experiences a change in pH and alters the type of polar groups absorbed; this leads to formation of negatively charged electrical double layers that attracts water molecules causing separation of asphalt from the aggregate (Ajay Ranka, 2014) (Kiggundu, 1988). This is also referred to as stripping of asphalt.

One of the products used as an antistripping additive is a nanoparticle Organosilane (Zydexindustries, 2015). Organosilane reacts with inorganic aggregate and modifies their surface. This modification improves the aggregates bonding with asphalt and increases the stripping resistance.

1.2 Objective

The objective of this study is to make the asphalt pavement production process more sustainable by using RAP, and also improve the moisture resistance of the material. One major goal is to evaluate the performance of asphalt pavements containing RAP with the Organosilane antistripping additive.

1.3 Scope

The scope of this study included City of Phoenix asphalt mixtures containing two percentages of RAP and using the Organosilane modified binder. Total two different RAP percentages were selected 15%, 25% in addition to a control mix (0% RAP). In total, six different types of mixtures were prepared with and without Organosilane (OS) as shown below:

- i. Control (0 % RAP)
- ii. 15% RAP
- iii. 25% RAP
- iv. Control + OS
- v. 15% RAP + OS
- vi. 25% RAP + OS

Mix designs were performed for control, 15% and 25% RAP dense graded mixes following City of Phoenix mix design specifications. Afterward, these mixes were modified by adding Organosilane. The use of OS did not require changes to the mix designs. Several samples were then prepared, at the optimum asphalt contents, and tested to determine the performance of the various mixes. Different performance tests conducted on the mixes were Dynamic Modulus, Flow Number, and moisture resistant test. The test results were compared between the mixes and conclusions were drawn from these results.

1.4 Organization of Report

The current thesis report is mainly divided into six chapters. Chapter 1 gives information about the background for the study, the objective and scope of work. Chapter

2, literature review, will discuss previous works related to this study, including different procedures followed in handling additives to the HMA like Organosilane and RAP.

Chapter 3 briefly presents the materials used in the current study and their properties.

Chapter 4, gives information about the tests and experiments conducted as part of the study. Chapter 5 includes the results and analysis. Chapter 6 summarizes the findings, conclusions, and gives recommendations for future works.

Chapter 2 Literature review

2.1 Recycled Asphalt Pavements

Recycled Asphalt Pavement (RAP) is the processed road milling that can be reused in road construction. Even though some states started using RAP, several states restricted the percentage of RAP in their HMA mixes due to concerns about the long-term pavement performance and lack of guidelines to use higher percentages of RAP (Copeland, 2011). Although several states are using up to 30% RAP in their intermediate and surface layers, the average usage in the United States is about 12%. A survey reported that the Long-Term Pavement Performance (LTPP) test sections throughout US and Canada with 30% RAP performed similarly to mixes without RAP (Copeland, 2011).

2.1.1 Studies on RAP mixes

Several studies were conducted on the usage of RAP, effect of RAP on volumetric and performance properties on the mix. The effect of RAP on the mechanical and volumetric properties of asphalt mixtures was studied by Daniel et al (Jo Sias Daniel, 2005). As part of the study, Superpave 19mm mixtures were prepared with varying RAP contents of 0%, 15%, 25% and 40%. Two types of RAP were used in the study, processed and unprocessed. The study summarized that Voids in Mineral Aggregate (VMA) and Voids Filled with Asphalt (VFA) of the mix increased for mixes with 25% and 40% RAP. The dynamic modulus values increased from 0% to 15% RAP, but the other two percentages of RAP showed similar behavior as the control mix. These trends were due to asphalt content, volumetric properties, and gradation.

Mohamady et al studied the behavior of RAP and its effect on the performance of asphalt mixture (Ahmed Mohamady, 2014). Six different percentages of RAP, 0%, 10%,

20%, 25%, 30% and 40% RAP samples were prepared by using Marshall mix design. The properties of the mixes were investigated through indirect tensile strength test and loss of stability. The study concluded that as RAP content increases the stability of mix decreases, which may be due to fatigue of aged materials. The mix flow increased by increasing the RAP content. Increasing recycled aggregate in the mix decreased the air voids which may lead to asphalt bleeding. The indirect tensile strength of the mix decreased and loss of stability of asphalt mix increased with increasing the RAP material.

Apart from laboratory studies, research also was reported on the long term and field performances of the RAP mixes. Anderson worked on the LTPP with high RAP content and analyzed several case studies (Anderson, 2012). In this study, several pavement sections with RAP content greater than 20% were placed and monitored for at least 10 years and compared with virgin mixtures of same age. The study reported that the sections with RAP performed comparably with the virgin mix. The high RAP sections exhibited low ride quality, a higher degree of cracking and high deterioration. However, when compared to the virgin mix, the lifespan was 5% less after 10 years of service, concluding that the RAP mixes were comparable to virgin mixes in long-term performance.

Al-Qadi et al conducted a study on the impact of high percentage of RAP on structural and performance properties of asphalt mixtures (Imad L. Al-Qadi, 2012). As part of the study, several mixes with 0%, 30%, 40%, 50% RAP were prepared with the base binder (PG 64-22), single-bumped binder (PG 58-22) and double-bumped binder (PG 58-28). The performance of these mixes was analyzed through complex modulus, flow number, moisture susceptibility, and beam fatigue tests.

The study concluded that the mix with up to 50% RAP was within specified limits for volumetric properties. To counteract the RAP stiffness, using double-bumped binder helped to retain the original virgin mix properties. The study recommended fractionating of RAP in HMA mixes for better performance; the binder grade should be double bumped when RAP greater than 30% was used to reduce thermal cracking and improve performance.

Fujie et al (Fujie Zhou, 2014) conducted a study on creating balanced RAP mix design system based on specific conditions of the project. The study concluded that RAP mixes can perform similar or better than virgin mixes, if the mixes were designed by balancing cracking, moisture damage and rutting. They also concluded that the cracking is not only influenced by RAP content but also affected by several other factors like traffic, pavement condition, structure, layer thickness etc.

A study was conducted on performance analysis of higher RAP mixes by Stimilli et al (Arianna Stimilli, 2017). HMA mixes with 40% RAP (fractionated) were prepared by modifying the binder with high and low percentage of SBS. The performance of these mixtures was compared to un-fractionated 25% RAP mix with unmodified binder. Bailey method was used for the mix design. The results concluded that the volumetric properties with 40%RAP were within limit and did not create any difficulty during compaction, which was contrary to the expectation. The 40%RAP mixtures with high modified SBS was stiffer than the reference mix; contrarily low modified SBS mix was less stiff than the reference mix and showed the best performance in fatigue resistance and ductility. It also showed optimum performance in terms of rutting because of improved aggregate

packing. The study recommended the use of a low modified binder when high amounts of RAP was used.

2.1.2 Handling RAP in the Laboratory

2.1.2.1 Sampling RAP

RAP is highly variable material and the stockpile at the asphalt plant may contain millings from several projects (Rebecca McDaniel, 2001). To reduce the variability of RAP, all the material in the stockpile should be mixed together and then processed. The typical sample size for testing RAP properties is 10kg, and for preparing samples for the Superpave mix design, the sample size should be at least 25kg.

2.1.2.2 Properties of RAP Constituents

The binder from RAP should be separated from aggregates and recovered for testing the characteristics of the binder. After extraction, knowing the amount of binder, the percentage binder present in the RAP material should be calculated to know asphalt content in the RAP. Several methods can be followed to separate the asphalt like centrifuge, vacuum, or reflux extractor using solvent. The binder solvent can be recovered either by using Abson method or Rotavapor where the solvent is boiled leaving the asphalt behind.

For the recovered binder, several classification tests need to be performed like Rotational Viscosity (RV), Dynamic Shear Rheometer (DSR) on recovered RAP binder, Rolling-Thin Film oven (RTFO), and Pressure Aging Vessel (PAV) aged recovered RAP binder to find the grade of RAP binder. The grade of asphalt blend with different percentage RAP and virgin binder need to be calculated for selecting the grade of virgin binder.

Gradation of RAP and extracted aggregate need to be determined to use the RAP in the mixes. Specific gravity, absorption of extracted aggregates and Theoretical Maximum Specific Gravity of RAP should be determined to use these values in preparation for RAP mix Design

2.1.2.3 RAP Drying and Heating

Before working with RAP, it needs to be dried completely. NCHRP Report 752 recommends 6 hours of heating at 110°C removes complete moisture (about 5.3%) from RAP material. Figure 2.1 shows the plot for moisture content in RAP against time at 110°C. (Randy West, 2013)

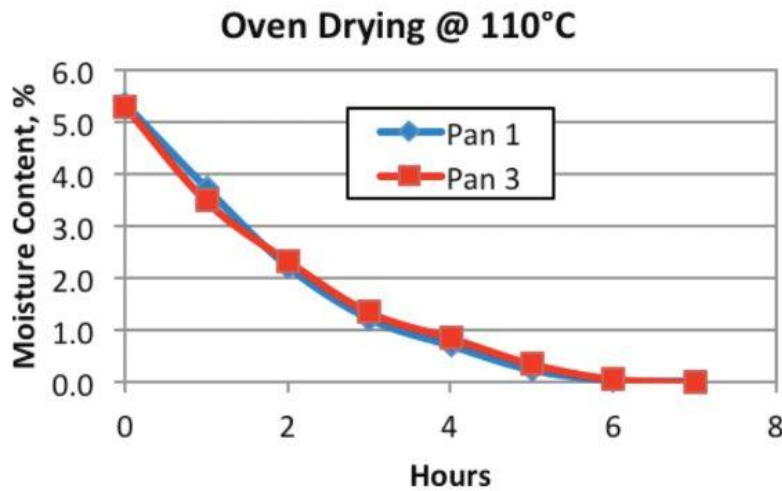


Figure 2.1 Moisture Content Changes for RAP dried in an Oven (Randy West, 2013)

Before introducing RAP into the HMA mix, it needs to be heated. There were several experiments conducted to determine the time and temperature that RAP needs to be heated. NCHRP 752 reported that it takes about 90 minutes for RAP sample to reach the set temperature and this value may vary depending upon the oven. The other scenarios were: 1) RAP and virgin aggregate heated together for 3 hours at 179°C; 2)

heating RAP and virgin aggregate together for 16 hours at 179°C; 3) heat virgin aggregate for 3 hours and RAP for 30 minutes at 179°C. 4) The aggregate was superheated to 260°C for 3 hours and RAP is not heated. Of these all four scenarios, RAP is least aged by following scenario three compared to others. Mix design steps need to be followed once RAP reaches the mixing temperature.

2.2 Warm Mix Asphalt

Warm Mix Asphalt (WMA) is the mix produced and compacted at a reduced temperature when compared to HMA and intended to give equivalent durability and strength as HMA. Generally, the mixing temperature range for HMA is 285°F to 340°F while for WMA it can be between 200°F to 275°F (Arif Chowdhury, 2008).

Chowdhury et al (Arif Chowdhury, 2008) reported on several WMA projects worldwide. Eight different WMA technologies were introduced in the USA. They are Asphaltan B, Sasobit, Low-energy Asphalt, REVIX, WMX, Double Barrel Green, WAM Foam and Aspha-Min. Some of these technologies performed better or comparable to HMA mixes. WMA reduced 30-50% fuel consumption, 30% of CO₂ emissions, 60% dust and 40% lesser fumes from paving machine. Due to lower mixing and compaction temperatures, incomplete drying of aggregate may take place and increases possibility of moisture damage. It also reported that RAP can successfully be incorporated into WMA mixes.

Zaumanis (Zaumanis, 2010) investigated WMA in Denmark. Different types of additives were added to the mix to prepare WMA mixes. It was observed that the change in Viscosity was smaller than expected for the modified binder. The compaction temperature used for the mixture was 125°C to get similar density as the HMA mix. The

stiffness of the mix and resistance to permanent deformation were reduced due to the reduction in compaction temperature. The study concluded that in some circumstances, WMA has advantages over HMA and can be used as a replacement for HMA.

2.3 Organosilane

Organosilane compounds react with inorganic material like aggregate and soil and modify their surface (Ajay Ranka, 2014). Ajay Ranka and Prakash Mehta conducted research on the chemistry of nano-based organosilane in HMA. Organosilane is the organo functional alkoxy silane. The alkoxy group is radical in the organic chain, which imparts required characteristics with polymers. This alkyl group may be Epoxy, Chloro, Mecapto, Amino etc. The alkyl group is used to impart the hydrophobic nature into the product. The silylating agents are used in the reaction between polymer and mineral to produce a composite which retains their properties in wet conditions. Thus, the interaction of this Organoalkyl silane converts hydrophilic aggregate to hydrophobic. Figure 2.2 shows Organosilane alkylalkoxy compound.

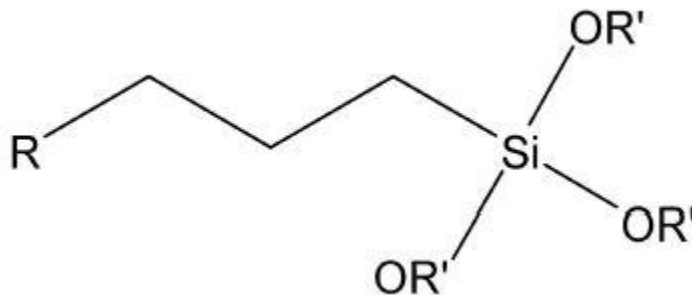


Figure 2.2 Organosilane alkylalkoxy compound (Ajay Ranka, 2014)

The hydroxy group present in the aggregate substrate forms a siloxane bond (=Si-O-Si=) with the alkoxy (OR') group present in the chain, which imparts hydrophobic nature to the aggregate surface. The possible reaction due to the interaction between substrate and Organosilane is shown below in Figure 3. All the reactions lead to the formation of the irreversible permanent Siloxane bond.

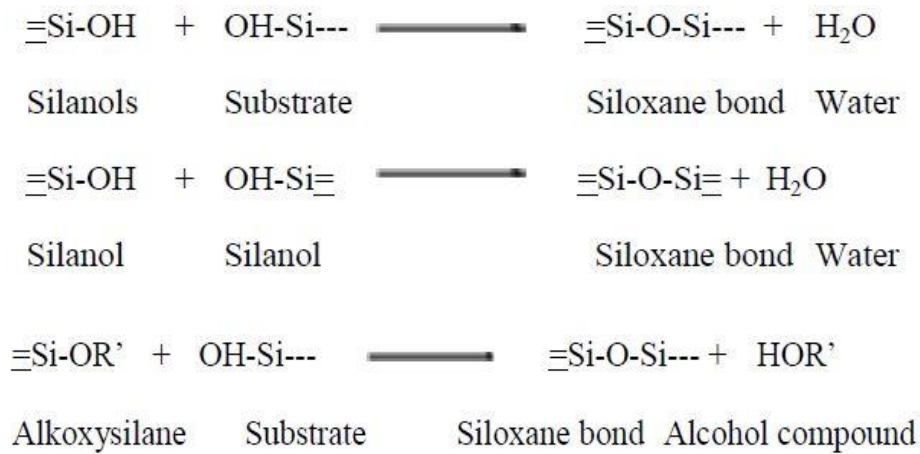


Figure 2.3 All possible reactions between substrate and Organosilane (Ajay Ranka, 2014)

This reaction changes the aggregate surface from hydrophilic to hydrophobic providing better bonding with non-polar asphalt in the mix. The silane reaction develops a nano-level organic interphase around the aggregate surface, which is suited for reaction with asphalt than highly polar -OH group. Due to this interphase, the microscopic surface air voids and air interphase around the aggregate surface are eliminated and provides complete wetting of aggregates. This air interphase around the aggregate is responsible for breaking the bond between asphalt and aggregate due to the intrusion of moisture. Thus, moisture resistance of the mixture is improved due to the elimination of this

interphase. Figure 2.4 shows the Organosilane reaction near the aggregate surface and formation of Siloxane bond with the aggregate surface.

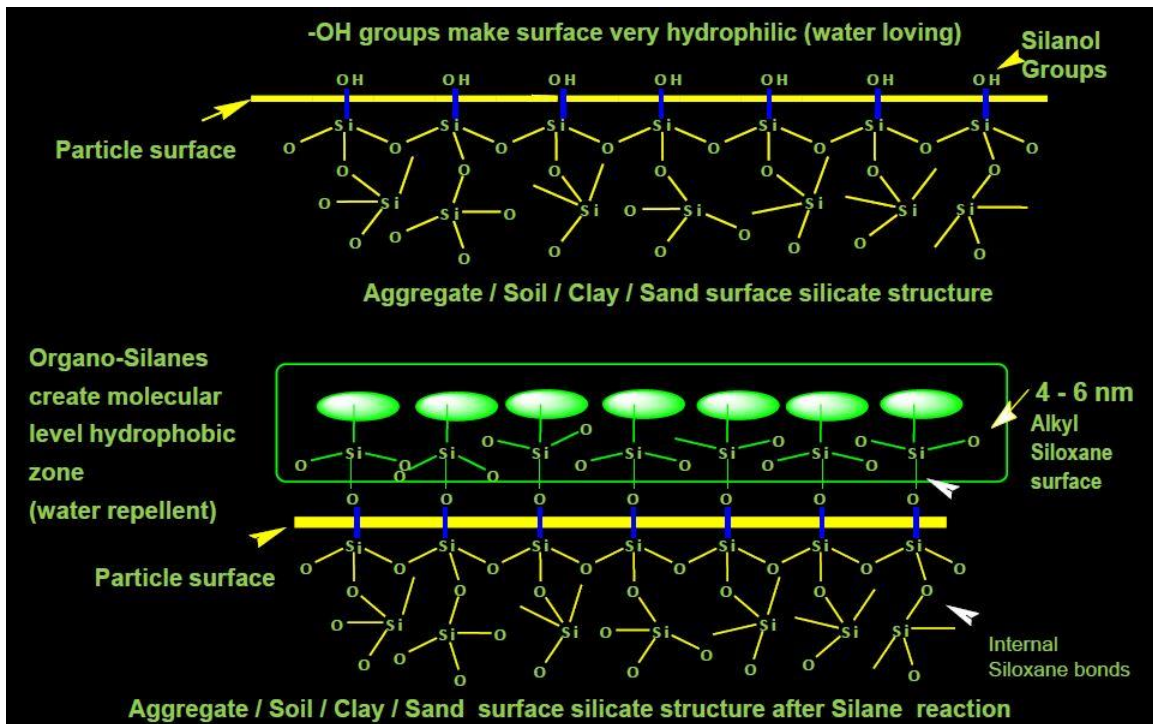


Figure 2.4 Silane reaction on aggregate surface (Ranka D. A., 2014)

The addition of Organosilane to asphalt mixtures involves two mechanisms, asphaltene capturing phenomenon and wetting phenomenon, which keeps actively working in the system (Ranka A. , 2018). Organosilane when added to RAP mixtures, it captures all asphaltenes and/or polar oxidized materials in a process that gets surrounded by non-polar tail, making them more compatible with the maltenes. The hardened oxidized material from RAP will get captured and transformed, and their interface at the aggregate leads to softening of mix. Organosilane are basically designed to transform aged, oxidized asphaltenes closer to a maltenes phase.

The RAP mix with OS is also expected to show better resistance to oxidation. This is due to lower surface tension created by OS in mix, which completely removes the

pinholes around the aggregate surface and makes the mix homogeneous. This is also referred to as wetting phenomenon.

Rohith and Ranjitha (Rohith N, 2013) conducted experiments on WMA prepared by addition of Zycotherm (ZT) which is an Organosilane (OS) product. The HMA mixtures were prepared at three different temperatures, 155°C, 130°C and 115°C, and two other mixtures by adding 0.1% ZT at mixing temperatures 130°C and 115°C. The study concluded that all of the mixtures with ZT performed better than other mixtures in Marshall Stability. The optimum binder content was also reduced slightly with the addition of ZT and varied with a change in dosage rate and temperature. The study recommended preparing WMA mix using 0.1% ZT at 130°C.

Zycotherm – a liquid and nano-Organosilane warm mix and anti-stripping additive, which is added to the asphalt mix (Mirzababaei, 2016). Mirzababaei used ZT and reported that it creates a Si-O-Si hydrophobic layer over the surface based on results from Fourier Transformed Infrared spectroscopy (FTIR). The study also reported that ZT significantly increased Tensile Strength Ratio (TSR), Resilient Modulus Ratio (RMR), Marshall Stability Ratio (MSR) and Fracture Energy Ratio (FER) values of mixtures. Although OS improves moisture susceptibility performance of mixtures, it does not function properly as WMA additive, as an effective additive should improve both unconditioned and moisture conditioned mixture performance.

Ayazi et al (Mohamad Javad Ayazi, 2017) conducted research on the influence of Sasobit and Zycotherm on properties of RAP- WMA. Results concluded that ZT mixtures had more resistance to moisture damage than HMA mixtures and WMA with Sasobit,

while the increase in mixture stiffness due to increasing in RAP amount is reduced by using Sasobit.

Raveesh and Manjunath (Raveesh J, 2017) studied the mechanical behavior of bitumen under the effect of ZT. The WMA produced by adding ZT to mix is compared to HMA. The study concluded that use of ZT in WMA reduced the mixing temperature and had given satisfactory results. The mix showed higher Marshall stability and moisture resistance than the HMA. WMA modified with ZT can become an alternative to HMA.

Hasan et al (Mohd Rosli Mohd Hasan, 2017) used 0.1% ZT by binder weight and prepared asphalt mixture at lower temperatures. By using ZT, better workability and compactability were achieved. As part of the study, cylindrical asphalt mixtures were produced by ZT modified binder using Servopac gyratory compactor and samples were tested for indirect tensile strength, resilient modulus, dynamic creep, Hamburg wheel tracing and moisture induced damage. The study concluded that, in terms of moisture damage, permanent deformation and cracking, the mixtures with ZT performed comparable if not better than control samples.

Chapter 3 Materials and Properties

3.1 Aggregate

In the current study aggregate used were from Southwest Asphalt El Mirage pit, Glendale, Arizona. The material was collected from different stockpiles sizes: 19 mm (3/4 “), 9.5 mm (3/8”), crushed fines and blend sand. The properties for the combined aggregates are shown in Table 3.1.

Table 3.1 Properties of combined aggregate

Property	Value
Bulk Specific Gravity	2.636
SSD Specific Gravity	2.671
Apparent Specific Gravity	2.731
Absorption (%)	1.321

In this study, a dense graded mixture with Nominal Maximum Aggregate Size (NMAS) of 19 mm (3/4”) was used. The gradation of the aggregate was selected following City of Phoenix specifications limits for gyratory compaction. The gradation used is shown in Table 3.2.

The aggregate stockpiles from the plant were heated at 110°C overnight to remove all the moisture from them before sieving them into different sizes. The dried aggregate then sieved and batched to the required weights. In Arizona, about 1% lime is added to all HMA mixtures and designs to reduce stripping potential.

Table 3.2 Gradation for Dense Graded Mix with NMAS 19 mm (3/4")

Sieves US	Sieve size (mm)	Cumulative % Passing	Cumulative % Retained	% Retained
1"	25	100	0	0
3/4"	19	100	0	0
1/2"	12.5	86	14	14
3/8"	9.5	72	28	14
1/4"	6.35	59	41	13
#4	4.76	56	44	3
#8	2.38	43	57	13
#16	1.19	32	68	11
#30	0.595	21	79	11
#50	0.397	11	89	10
#100	0.149	6	94	5
#200	0.075	4.8	95.2	1.2
Pan				3.7
Lime				1.1
				100

3.2 Asphalt Binder

The binder for this study was provided by Western Refining company and the grade of the binder used was Performance Grade PG 70-10. The properties of the binder are shown in Table 3-3.

Table 3.3 Properties of PG 70-10 Asphalt Binder

Property	Value
Mixing Temperature	157°C- 163°C
Compaction Temperature	147°C-151°C
Viscosity (cP) at 135°C	560
Viscosity (cP) at 175°C	96
Specific Gravity @60F	1.0244
Specific Gravity @77F	1.0184

3.3 Recycled Asphalt Pavement

The processed RAP milling was supplied by Southwest Asphalt plant, El Mirage pit, Glendale, Arizona (see Figure 3-1). The binder and aggregates from the RAP was extracted and recovered for testing.



Figure 3.1 Processed RAP material at Southwest Asphalt, El Mirage Plant

Tests were conducted on the extracted binder for finding the Performance Grade by Arredondo et al. as part of City of Phoenix project at Arizona State University (Gonzalo Arredondo, 2017). The results showed that the RAP has an average binder content of 3.8% and PG 112 + 14.

Sieve analysis of RAP millings and extracted aggregate were conducted by following AASHTO T30. Wet sieve analysis was also performed to find the dust percentage in the material. The findings from this analysis was tabulated and shown in Table 3.4. Comparison plots are shown in Figure 3.2.

Table 3.4 Gradation Comparison of RAP and Extracted RAP Aggregate with City of Phoenix Limits (Phoenix, 2015)

Sieve Size (in.)	Sieve Size ^{0.45} (mm)	City standards		Southwest Plant Sample			
		Upper Limit	Lower Limit	RAP	RAP washed	Extracted Aggregate	Washed Extracted Aggregate
1	4.26	100	100	100	100	100	100
3/4	3.76	100	100	100	100	100	100
1/2	3.12	100	90	89	89	91	90
3/8	2.75	89	53	77	76	77	76
#8	1.48	40	29	28	27	36	32
#40	0.68	20	3	7	6	14	9
#200	0.31	7.5	2	1	0	4	0
Dust Percentage (%)				1.86		5.59	

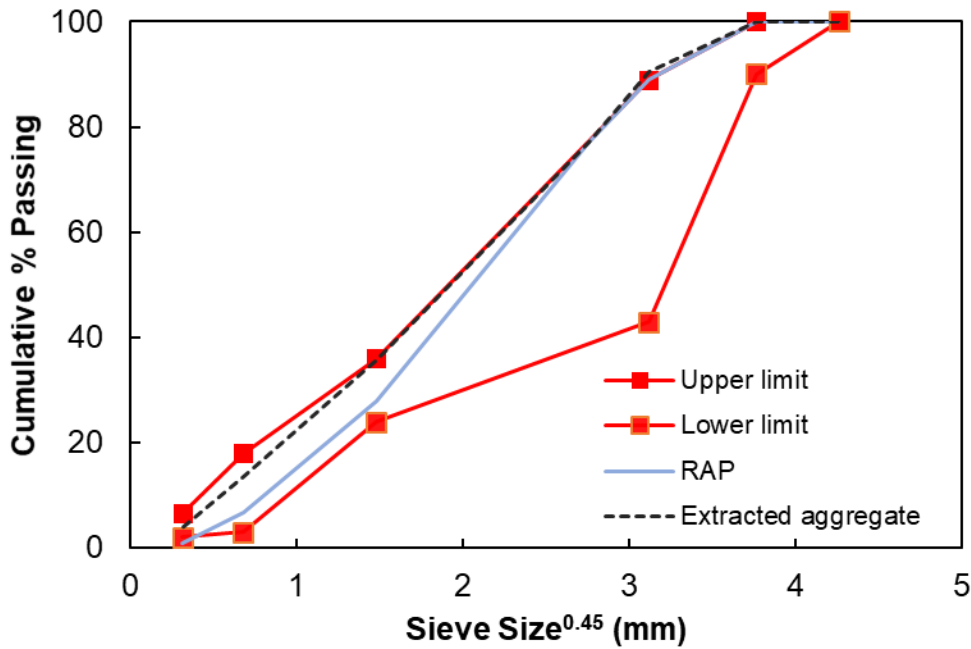


Figure 3.2 RAP and Extracted Aggregate Gradation.

The specific gravity of the extracted RAP aggregates was found by using AASHTO T 85 for coarse aggregate, and AASHTO T 84 for fine aggregate. Aggregates

were separated by using 4.76 mm (No. 4) sieve. The material retained on 4.76 mm (No. 4) sieve is coarse aggregate and the aggregate passing 4.76 mm (No. 4) is fine aggregate. The specific gravity values are shown in Table 3.5.

Table 3.5 Specific Gravity values for extracted RAP aggregate

Property	Coarse Aggregate	Fine Aggregate
Bulk Specific gravity (Gsb)	2.60	2.60
Gsb SSD	2.63	2.64
Apparent Specific gravity	2.69	2.72
Absorption %	1.29	1.62

Based on literature, and to find out the time required for RAP material to reach the mixing temperature, RAP was heated at 163°C separately in one case and heated along with the virgin aggregates (already at 163°C) in another case (Figure 3.3). The case-1 showed, 90 minutes of heating is required for RAP material to reach the mixing temperature, but the melted binder adhered to the walls of container. Case-2 showed that when RAP aggregate was placed on hot aggregate, one hour of heating was sufficient as heat from aggregate also helped to raise the temperature of RAP.



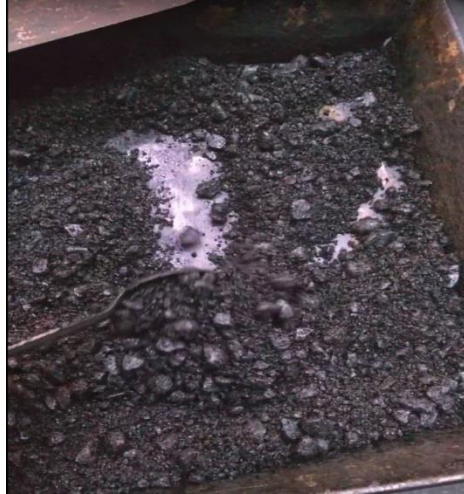
Figure 3.3 Experiments of heating RAP before mixing, left photo case-1, right photo case-2.

For this study, heating RAP by placing it on hot aggregate for one hour was followed, and care taken to avoid the contact between the RAP and container to avoid the loss of melted RAP binder by sticking to walls of the container.

3.4 Organosilane

As discussed in Chapter 2, Organosilane is the Organo functional alkoxy silane. In the current study Organosilane (OS) used was Zycotherm which is prepared by using 3C nanotechnology by Zydex Industries, Vadodara, India. OS is an anti-stripping additive that should be stored at 5-45°C.

The specific gravity of OS is near to 1, which means 1 ml of OS is equal to 1 gm (Zydexindustries, 2015). The mixing temperature was recommended to be reduced by 10°C-15°C, and compaction temperature to 30°C-40°C when OS is added to mix. In this study, when OS was used, the mixing temperature was reduced to 153°C and compaction temperature to 121°C compared to those values shown in Table 3-3. These temperatures also make the mix as Warm Mix Asphalt. OS also reduced the stickiness of the binder (asphalt) to the metal container as shown in Figure 3.4.



(a)



(b)



(c)

Figure 3.4 Cleaner equipment due to non-sticky nature of OS modified binder

3.4.1 Dosage of OS

The dosage of OS used depends upon several things like aggregate type, binder type and modifications to mix. The dosage recommended, in terms of % by weight of asphalt binder (Virgin+ Extracted), for different percentages RAP in the mix is shown in Table 3.6 below (Zydex, 2014).

Table 3.6 Dosage of OS depending on the type of Mixture

RAP %	% OS by weight of binder
<20%	0.080
25%	0.088
35%	0.100
45%	0.125

3.4.2 Mixing of OS to Binder

The dosage of OS to be mixed with the binder is relatively small. Assuming OS dosage rate as 0.1%, for 1000 gm of binder, 1 gm (equal to 1 ml) of OS is required. A dry and disposable 1 or 5 ml syringe was used to add drops of OS to the binder. The binder and OS were mixed at 150°C by using mechanical stirrer which is capable of producing 20 to 30 mm deep vertex in asphalt (Figure 3-5). OS was added at 10 drops per minute in center of the vertex as shown in Figure 3.6 while stirrer speed is constant and should be left stirred for 5-10 minutes for complete mixing after adding OS.



Figure 3.5 High shear mixer



a) OS liquid



b) Adding OS

Figure 3.6 Adding OS to asphalt at 150°C

The equipment used was high shear mixer shown in Figure 3.5. The asphalt is heated and maintained at 150°C before adding OS. The stirrer is set to a speed of 1500 rpm before addition OS and raised to 2500 rpm at the time of adding OS. As mentioned before, OS is added at the speed of 10 drops per minute. After completion of adding OS, stirrer speed was raised to 5000 rpm and mixed for 10 minutes assuring complete mixing. After mixing, the binder was added to aggregate when both are at mixing temperature, to continue the preparation of the asphalt mixtures.

A small study was conducted on the Organosilane modified binder and results were compared to the virgin binder. The viscosity and Dynamic Shear Rheometer tests were conducted on unaged binder.

The viscosity test was conducted on Organosilane modified and unmodified binder at 135°C and 165°C. The results showed there was no significant effect of Organosilane on the viscosity of the binder; both the binders showed similar results. Figure 3.7 shows the viscosity-temperature relationships for the two binder with almost identical results.

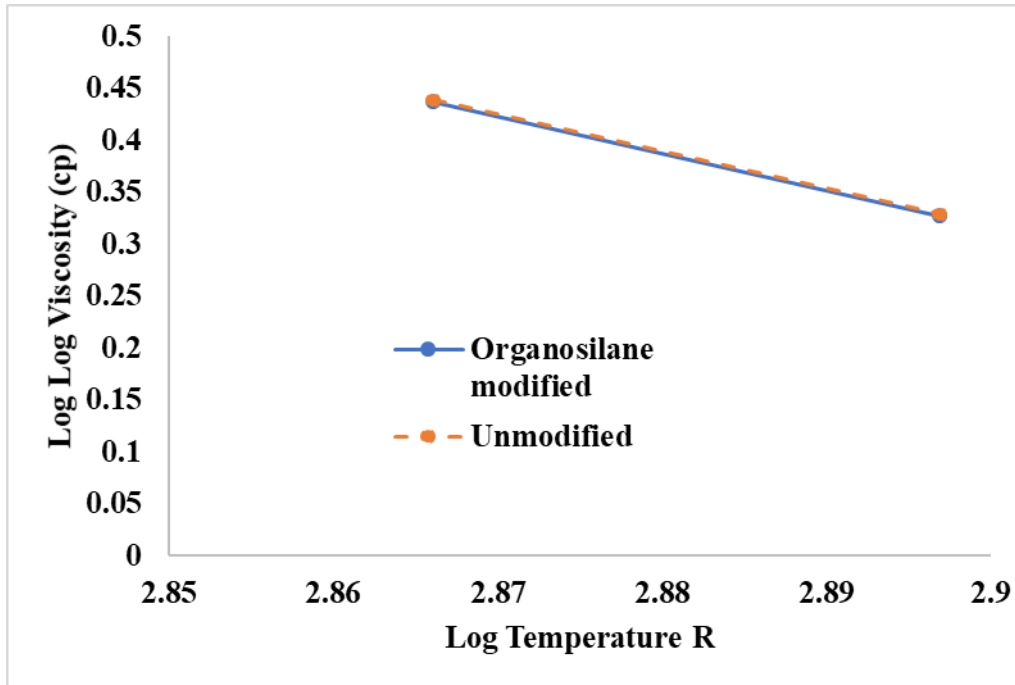


Figure 3.7 Viscosity of Organosilane modified and unmodified binders at different temperatures

The Dynamic Shear Rheometer (DSR) was used for characterizing the viscous and elastic behavior of asphalt at different temperatures. The DSR test gives information about the complex modulus (G^*) and Phase angle (δ) of the binder. This data can be used to predict the behavior of rutting and fatigue cracking. The test was conducted at three temperatures and the results are tabulated in Table 3.7.

Table 3.7 Dynamic shear Rheometer test results for Organosilane modified and unmodified binders

Sample:	PG 70-10+OS				PG 70-10			
	Temp. [C]	G*	Phase angle (degrees)	G*/Sin(P A)	G* *sin(P A)	G*	Phase angle (degrees)	G*/Sin(P A)
64	2.86	87.41	2.864	2.858	3.01	87.33	3.015	3.008
70	1.27	88.35	1.271	1.270	1.33	88.26	1.326	1.325
76	0.60	89.11	0.599	0.599	0.62	88.86	0.619	0.619

The $|G^*| \sin(\delta)$ and $G^*/\sin(\delta)$ values are used to evaluate the fatigue and rutting behaviors, respectively. $G^*/\sin(\delta)$ is used to assess the rutting behavior. The higher $G^*/\sin(\delta)$ value means higher resistance for rutting. $|G^*| \sin(\delta)$ used to assess the fatigue behavior. Lower $|G^*| \sin(\delta)$ is good for fatigue resistance.

From the table, the $|G^*| \sin(\delta)$ and $G^*/\sin(\delta)$ are lower for OS mix when compared to mix without OS. Based on this limited testing, an asphalt mixture with OS modified binder would perform better in fatigue; but an asphalt mixture without OS would perform better in rutting.

Chapter 4 Experimental procedure

4.1 Mix design

Mix design is the simulation of finding appropriate percentages of aggregate and asphalt contents, which gives the best performance mixture. (HMA Mix Design Fundamentals, 2012). In this study, RAP mix designs were prepared by following NCHRP Report 452 (Rebecca McDaniel, 2001).

4.1.1 Mixing

- i. The virgin aggregate dried overnight and sieved into different sizes. The sieved aggregate was batched according to gradation.
- ii. RAP aggregates were fractionated into the needed sizes and batched separately to the required amounts based on the percentage of RAP used in the mix. For example: if 10% RAP mix needed to be designed, 90% of the aggregate is virgin aggregate and 10% is from RAP.
- iii. Virgin aggregate was heated to 163 °C for 5 hours to reach the mixing temperature (Figure 4-1). If OS was used, the mixing temperature reduced to 153°C. Before one hour of mixing, RAP aggregate was placed on the aggregate without touching the walls of the container.



Figure 4.1 Heating aggregate at mixing temperature

- iv. Based on the binder content in the RAP, the virgin asphalt was reduced depending upon the percentage of RAP used. For example: if 5% is the selected binder content, RAP has 4% binder and 10% RAP is used in the mix, then binder contribution from RAP is $0.1 * 4 = 0.4\%$; and amount of virgin asphalt that is added is 4.6%.
- v. The binder was heated to the mixing temperature. When OS was used in the mixture, binder and OS were mixed at 150°C as discussed in the previous chapter. Then the modified was heated to mixing temperature.
- vi. Samples with three different binder contents were prepared with a difference of 0.5% (4.5%, 5%, 5.5%). Two replicates at each binder percentage were prepared.
- vii. The mix design samples were prepared for a mixture weight of 4700 gm. After adding the binder to aggregate, both were mixed for 90 seconds for complete coating as shown in Figure 4.2.



Figure 4.2 Mixing of aggregate and binder

- viii. After mixing, the sample was spread flat on the pan (Figure 4-3) and short term aged for 2 hours at the compaction temperature.



Figure 4.3 Spreading the HMA flat on pan for short term aging

- ix. The mixture was then transferred to the compaction mold along with base plate that were preheated in the oven and placed back in the oven until it reached the compaction temperature for a period of 30 to 60 minutes.

- x. Using gyratory compactor (Figure 4-4), samples were compacted to N_{max} gyrations. For the current study, N_{max} is 115 based on the City of Phoenix specifications.



Figure 4.4 Gyrotory compactor

4.1.2 Theoretical Maximum Specific Gravity (G_{mm})

- i. The samples were prepared by following the same steps up to step- viii in section 4.1.1. The procedure for this test was followed using (AASHTO-T209, 2016).
- ii. The samples were cooled down to room temperature and 2500 gm (A) of the sample placed into vacuum container with water level covering the sample.
- iii. The entrapped air from the sample was removed by gradually increasing vacuum till the pressure inside shows reading of 27.5+/-2.5 mm of Hg for 15 min. Mechanical agitation was used during vacuum period.

- iv. After 15 min, the vacuum was released, and the container was completely filled with water without any air bubble inside and weighed (B).
- v. The weight of container completely filled with water was determined (C)
- vi. G_{mm} was calculated by using the following equation:

$$G_{mm} = \frac{A}{A + C - B}$$

4.1.3 Bulk Specific Gravity of Compacted Hot Mix Asphalt (G_{mb})

- i. The specimen prepared from gyratory compaction was cooled to room temperature for overnight. The procedure for this test was followed using (AASHTO-T166, 2016)
- ii. The dry mass of the sample was recorded (A). The sample was immersed in water bath at 25°C for 4 +/- 1 min. Record the immersed mass (C).
- iii. Record the surface dry weight of the sample by quickly blotting sample with a damp towel (B)
- iv. The bulk specific gravity of specimen and absorption by specimen were calculated using the equations:

$$G_{mb} = \frac{A}{B - C}$$

$$Absorption \% = \frac{B - A}{B - C}$$

4.1.4 Mix design calculations

- i. The height of compacted specimen at N_{int} , N_{dsg} and N_{max} was recorded and G_{mb} was estimated by knowing the mass of the sample.

$$G_{mb} \text{ (estimated)} = \frac{\frac{M_{mb}}{V_{mx}}}{\rho(\text{water})}$$

- ii. N_{int} , N_{dsg} and N_{max} in the current study were 7, 75 and 115. Volume at each gyration was calculated using the height at that gyration. The diameter of the samples was 150mm.

$$V_{mx} = \pi * d^2 * h_x * \frac{0.001}{4} \text{ cm}^3/\text{mm}^3$$

- iii. Correction factor was calculated by taking ratio of measured G_{mb} to estimated G_{mb} at final height.

$$C = \frac{G_{mb} \text{ (measured)} @ N_{max}}{G_{mb} \text{ (estimated)} @ N_{max}}$$

- iv. The estimated values of G_{mb} at other two gyration levels were corrected by multiplying the values with correction factor.
- v. At all the gyration levels % G_{mm} was calculated

$$\%G_{mm} = \frac{G_{mb} \text{ (corrected)}}{G_{mm}} * 100$$

- vi. Air voids for each specimen at N_{dsg} were calculated

$$P_a = 100 - \%G_{mm} @ N \text{ (dsg)}$$

- vii. Percentage binder required to achieve 4% air voids was calculated by using the plot between binder content and air voids.

- viii. Other volumetric properties at optimum binder content were calculated and compared with the Superpave criteria.

$$VMA = 100 - \frac{\%G_{mm} @ N(dsg) * G_{mm} * R_s}{G_{sb}}$$

$$\text{Where } R_s = \frac{P_s}{100}$$

$$VFA = 100 * \frac{VMA - Pa}{VMA}$$

$$Dust\ Proportion = \frac{P_{0.075}}{P_{be}}$$

Where $P_{0.075}$ = percentage aggregate passing 0.075 mm sieve

P_{be} = effective asphalt content

4.2 Performance tests

4.2.1 Sample preparation

- i. The HMA mixture was prepared in the same way as discussed in 4.1.1. The mixture was aged for 4 hours before compacting at 135°C.
- ii. The mass required to achieve the target air voids were calculated knowing G_{mm} of the mix. Trial samples were fabricated varying the mass around estimated value. The samples were cored and cut into the required size and air voids of the samples were determined. From the air voids values of these trial samples, the mass required to obtain the target air voids was calculated.
- iii. Samples were fabricated by using the determined mass in step ii. For the performance testing, cylindrical samples of diameter 150mm and height 180mm were compacted.
- iv. The test samples needed were cored and cut to size with diameter 100 mm and height 150 mm for dynamic modulus and flow number tests as shown in Figure 4.5. For indirect tensile strength test, the test samples were cut to a thickness of 63 mm.



Figure 4.5 Specimen cored and cut from compacted size to required size.

- v. The samples were reduced to the required size by using coring and cutting machines.
- vi. Once the samples were reduced to required size, they were dried, and air voids were calculated.
- vii. For dynamic modulus and flow number tests, the samples needed to be instrumented before testing in the AMPT.
- viii. The buttons were glued to the samples to fix the instrumentation (mounting studs) for axial LVDT's for testing. The gauge length should be 70 mm \pm 1 mm center to center between gauge points. The schematic diagram was shown **Figure 4.6 Schematic of gauge points for dynamic modulus and flow number samples** Figure 4.6. In the present study three LVDT's were used to record the deformations when the load applied.

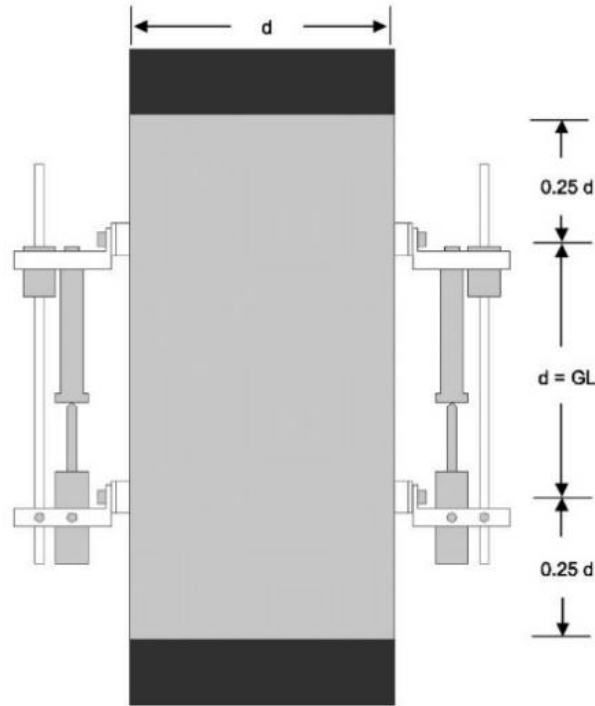


Figure 4.6 Schematic of gauge points for dynamic modulus and flow number samples (AASHTO-TP79-15, 2016)

- ix. Greased double latex friction reducers were used on both ends with size slightly larger than the loading platen to reduce the friction while testing.

4.2.2 Dynamic Modulus

Dynamic Modulus is the basic property of HMA mixture which gives information about the stiffness of the mixture in terms of temperature and time (Witczak M.W, 2002). The Mechanistic-Empirical Pavement Design Guide (MEPDG) uses the information from a master curve obtained from the results of the dynamic modulus.

The master curve is used to predict the viscoelastic properties of asphalt sample over a wide range of frequencies and temperatures (Witczak M.W, 2002) (Abbas Booshehrian, 2013). The master curve is generated using the stiffness values at five temperatures (-

10°C), 4.4°C, 21.1°C, 37.8°C, 54.4°C and at six frequencies at each temperature 25Hz, 10Hz, 5 Hz, 1 Hz, 0.5Hz, 0.1Hz.

In this study, Asphalt Mixture Performance Tester (AMPT) machine was used for the test. The test generates the mix stiffness value at all six frequencies at a given temperature. Three specimens were tested at all five temperatures and the average value of the three was considered for generation of the master curve. The test was conducted by following AASHTO T 342 (AASHTO-T342, 2011). The procedure is as follows:

- i. The specimen to be tested was assembled with friction reducers between loading platens and specimen on both the ends.
- ii. The specimen was placed inside environmental chamber along with dummy sample to monitor the temperature.
- iii. The specimen was mounted with the deformation measuring systems which were calibrated within range (Figure 4-7).



Figure 4.7 Specimen for dynamic modulus testing.

- iv. In the dynamic modulus software, sample information and other required information was entered, and test was started. The AMPT will automatically unload when the test was completed and generates the data.
- v. By using the generated results at five temperatures and six different frequencies, master curves were generated.

The modulus values obtained from the test were plotted against the log of reduced time or frequency. The values at all temperatures were shifted to one reference temperature using the shifting equation. The sigmoidal equation for the master curve was generated with curve fitting parameters by trial and error method reducing the error between the measured and predicted modulus values.

$$\text{Shifting equation: } \log a(T) = aTi^2 + bTi + c$$

$$\text{Sigmoidal equation for modulus: } \log|E^*| = \delta + \left(\frac{\alpha}{1 + e^{\beta + \gamma(\log tr)}} \right)$$

Where a,b,c,α,β,γ,δ are the fitting parameters determined by using the measured values.

4.2.3 Flow Number

The Flow Number (FN) is one of the performance tests relates to rutting resistance of asphalt mixtures. The FN is measured using repeated load testing. In this test, haversine axial compressive load pulses are applied to the specimen (Witczak M.W, 2002) (Bonaquist, 2012). The test was conducted following (AASHTO-TP79-15, 2016).

The test procedure is summarized below:

- i. The specimen was instrumented similar to the dynamic modulus test.
- ii. The specimen was placed inside the environmental chamber with greased double latex friction reducers between loading platens on both ends.

- iii. The specimens were mounted with the deformation measuring systems which were calibrated within range (Figure 4-8).
- iv. The AMPT was turned on with the set temperature of 50°C. The test was started once the sample reached the test temperature.
- v. Required information was input into the FN software such as specimen identification and control information.
- vi. The AMPT will automatically unload once test was completed and generates the output.



Figure 4.8 Flow number testing for sample

From the data, FN is the cycle number at which the tertiary stage is reached, when the rate of change of permanent strain reaches the minimum value. This value can be found by differentiating the permanent strain versus the load cycles. Figure 4-9 shows a sample after the test.



Figure 4.9 Flow number sample after completion of test

Several models were developed for predicting the flow number value. The Franken model is one that is used to calculate the FN. The approach uses the permanent strain values at each cycle to fit the Franken model. The equation is shown below

$$\varepsilon_p = An^B + C(e^{Dn} - 1)$$

In this equation, A, B, C, D are the fitting coefficients. Using numerical optimization, these coefficients are determined. First and second derivatives of the above equation are derived. Flow number is the cycle where the second derivative of this equation changes its sign from negative to positive. The derivatives of this equation are shown below.

$$\frac{d\varepsilon_p}{dn} = ABn^{B-1} + CD e^{Dn}$$

$$\frac{d^2\varepsilon_p}{dn^2} = AB(B-1)n^{B-2} + CD^2 e^{Dn}$$

The flow number can also be predicted by using the volumetric properties of mix and other parameters shown below (Rodezno M.C, 2010).

$$\log FN = 0.485 + 0.644 \log V_1 + 0.0874P(200) - 3.323 \log p + 0.0129 R(04) \\ - 0.0803Va + 2.593 \log q - 0.0142 R(34)$$

Where FN is flow number

V_1 = Binder Viscosity at testing temperature

P (200) = Percentage passing No. 200 sieve

R (04) = Percentage retained in No.4 sieve

R (34) = Percentage retained in ¾ in. sieve

p (psi) = Average Normal Stress

q (psi) = Maximum shear stress

A rutting prediction model was developed (Maria C. Rodezno, 2013) which predicts the possible amount of rutting using the flow number value, number of ESAL's and thickness of the layer. The model is

$$R = 0.0038 * FN^{-0.242} * ESALs^{0.485} * h^{-1.021}$$

Using the above model, potential rutting was also calculated for the various mixtures assuming a layer depth and number of ESALs. The rutting values from all the mixtures were compared.

4.2.4 Tensile strength Ratio

Tensile Strength Ratio (TSR) is the ratio of indirect tensile strengths of samples which underwent freeze-thaw cycle (conditioned samples) to the dry samples (unconditioned samples). In this study, TSR of all six mixtures was tested by following AASHTO T 283 (AASHTO-T283, 2016) and reported. A summary of the process is as follows:

- i. The Samples were prepared by following procedure discussed in 4.1.1.

- ii. The samples were cored and cut to a diameter of 100 mm and thickness of 63 mm.
- iii. Six samples of each mix were prepared, three for conditioned testing and three for unconditioned testing.
- iv. Air voids for all the samples were calculated in accordance with T 269.
- v. The specimens were grouped into two subsets with approximately same air voids. One of the subsets was conditioned.
- vi. After conditioning both the subsets were placed in sealed plastic bags and placed in water bath at 25°C for 2 hours.
- vii. After 2 hours, the specimens were removed from water and thickness was noted.
- viii. The specimens were placed between loading strips and entire arrangement was placed between bearing plates in testing machine. The load was applied at a rate of 50 mm/min (Figure 4-10).
- ix. The load applied for the maximum strength was noted from the testing machine and the strength was calculated as follows

$$Strength = 2000 * \frac{Load}{\pi * t * D} \text{ kPa}$$

- x. The ratio of strengths of conditioned and unconditioned samples was calculated and reported as tensile strength ratio of the mixture.



Figure 4.10 Indirect tensile strength test

Conditioning of Samples

- i. One of the subsets were conditioned to test indirect tensile strength.
- ii. The specimens were subjected to vacuum saturation with a minimum of 25mm water level above the specimens.
- iii. Vacuum of 13 to 67 kPa (10 to 26 in. Hg partial pressure) absolute pressure was applied for 5 to 10 min. Then Vacuum was removed, and sample left submerged for 5-10 min.
- iv. The surface saturated dry mass (B' gm) of the vacuum saturated was recorded and percentage saturation (S') was calculated by knowing the dry weight (A gm.) of the specimen.

$$S' = 100 * \frac{(B' - A)}{Va}$$

where, Volume of air voids $Va = Pa * \frac{E}{100} cm^3$

E is the volume of specimen in cm^3 and Pa is the percentage air voids in specimen.

- v. The degree of saturation between 70 to 80 percent were targeted. Once the sample is in this saturation range, the procedure continued
- vi. The specimens were wrapped tightly with plastic film and were placed into the plastic bag with 10 ml of water in it and were sealed and cooled at -18°C for a minimum of 16 hours.
- vii. Later the samples were placed in the water bath maintained at 60°C with at least 25 mm water above the specimen surface for 24 ± 1 hours and removed.

Chapter 5 Results and Analysis

5.1 Mix design

By following the procedure described in Chapter 4, the mix design was performed for all three RAP mixtures; and mixtures with OS were prepared with optimum binder content. All the results for the mix designs of 0%, 15% and 25% RAP mixtures are shown in Table 5.1,

Table 5.2, Table 5.3, respectively. The results were also compared with the specification limits. The mix design calculations were shown in APPENDIX A.

Table 5.1 Volumetric properties of 0% RAP mix

	Criteria	Result	Specifications
Mix Property	3/4" Mix		
Asphalt Binder (%)		5.02	
Air Voids (%)	4.0+/-0.2	4.00	
VMA (%)	13 min.	14.76	Pass
VFA (%)	65 - 78	72.59	Pass
Absorbed Asphalt (%)	0 - 1.0	0.38	Pass
Dust Proportion	0.6 - 1.4	1.03	Pass
%Gmm@Nini = 7	less than 90.5	89.4	Pass
%Gmm@Nmax =115	less than 98	97.0	Pass

Table 5.2 Volumetric properties of 15% RAP mix

	Criteria	15%RAP	Specifications
Mix Property	3/4" Mix		
Asphalt Binder (%)		5.37	
Air Voids (%)	4.0+/-0.2	4.00	
VMA (%)	13 min.	13.45	Pass
VFA (%)	65 - 78	70.33	Pass
Absorbed Asphalt (%)	0 - 1.0	0.30	Pass
Dust Proportion	0.6 - 1.4	0.94	Pass
%Gmm@Nini = 7	< 90.5	89.3	Pass

%Gmm@Nmax = 115	< 98	96.9	Pass
-----------------	------	------	------

Table 5.3 Volumetric Properties of 25% RAP mix

	Criteria	Result	Specifications
Mix Property	3/4" Mix		
Asphalt Binder (%)		5.75	
Air Voids (%)	4.0+/-0.2	4.00	
VMA (%)	13 min.	15.10	Pass
VFA (%)	65 - 78	74.79	Pass
Absorbed Asphalt (%)	0 - 1.0	0.25	Pass
Dust Proportion	0.6 - 1.4	0.87	Pass
%Gmm@Nini = 7	less than 90.5	88.8	Pass
%Gmm@Nmax = 115	less than 98	97.0	Pass

Basically, after calculating the air voids for all replicates with different binder contents, the binder content which gives 4% air voids was determined by plotting the %air voids against % binder contents for all replicates. This binder content is reported as the Optimum Binder Content, which was used to prepare further samples for each mix. All other volumetric properties were calculated at this binder percentage and compared to the specification limits. For all three mixtures, the volumetric properties were within the passing limits.

The volumetric properties of all three RAP mixtures were compared and shown in Table 5.4 to check the effect of RAP on the properties. From this table, it can be observed that at 4% air voids, the asphalt content for the mixtures increased with increasing RAP content, as expected. VMA% and VFA% decreased at 15% RAP content, but the mix with 25% RAP has higher VMA% and VFA%. The absorbed asphalt content decreased

with increasing RAP content as the mix with RAP absorbs less due to the presence of old binder on some of the aggregate. The dust proportion of the RAP mixtures was less as some of the dust was held by the old binder from RAP.

Table 5.4 Comparison of all the volumetric properties of RAP mixes

Mix Property	%RAP		
	0%	15%	25%
Asphalt Binder (%)	5.02	5.37	5.75
Binder from RAP	0	0.57	0.95
Virgin binder added	5.02	4.8	4.80
Air Voids (%)	4.00	4.00	4.00
VMA (%)	14.76	13.45	15.10
VFA (%)	72.59	70.33	74.79
Absorbed Asphalt (%)	0.40	0.30	0.25
Dust Proportion	1.03	0.94	0.87
%Gmm@Nini = 7	89.42	89.34	88.76
%Gmm@Nmax = 115	97.01	96.94	97.02

The samples were prepared at optimum binder content for each mix by adding OS to the mix to check the effect of OS and reduction in temperature to the mix. The results are shown in Table 5.5 which shows a decrease in air voids by addition of OS. The compaction curve for mix with and without OS was plotted and shown in Figure 5.1. Despite the lower compaction temperature for the OS mixture, the OS enabled higher compaction, which needs to be considered in future studies and paving processes.

Table 5.5 Effect of OS on air voids of mix

RAP %	0%	15%	25%
Binder content	5.02	5.37	5.75
OS%	0.080	0.080	0.088
Air voids%	3.75	3.82	3.87

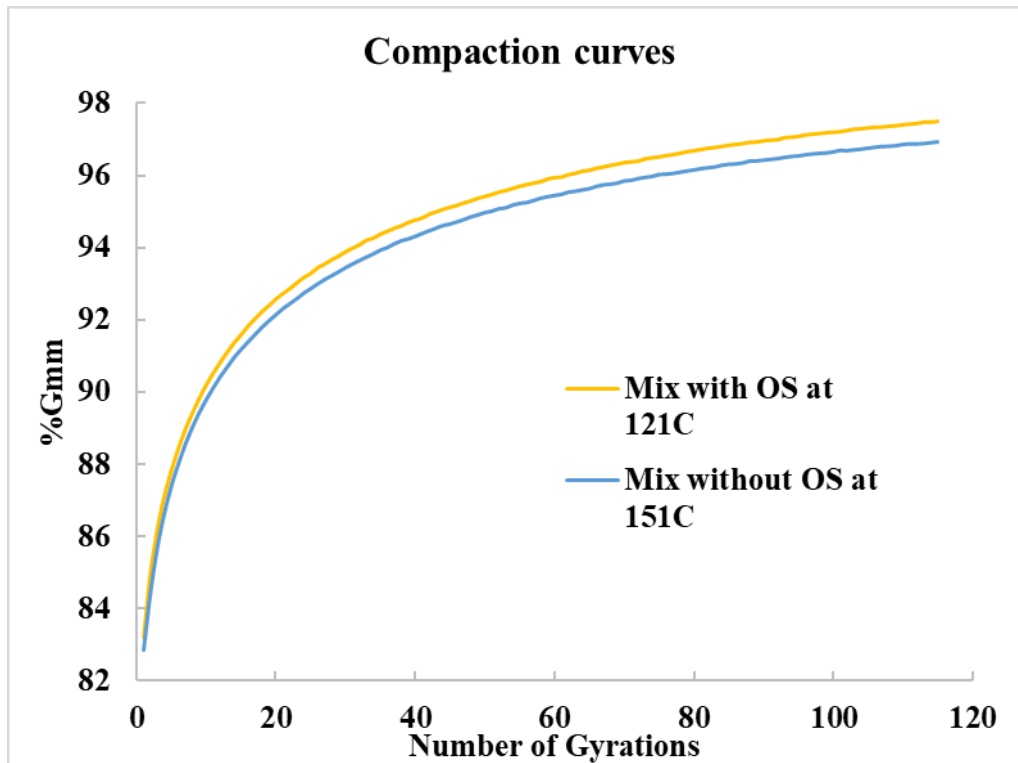


Figure 5.1 Comparison of Compaction curves with and without OS

5.2 Dynamic modulus

The dynamic modulus test was conducted at all five temperatures with six frequencies at each temperature. From the results, master curves were prepared by shifting the modulus values to one reference temperature. The results from dynamic modulus test for all the replicates of all the mixtures and coefficient of variation (cv%) between replicates were shown in APPENDIX B. The cv% values were below 31% as specified in AASHTO TP 79. The fitting coefficients, shifting coefficients for all the mixtures are shown in Table 5.6.

Table 5.6 Parameters for sigmoidal equation of dynamic modulus determined from Master curve

Parameter	0% RAP	0% RAP+OS	15% RAP	15% RAP+OS	25% RAP	25% RAP+OS
δ	3.0725	3.1118	3.3499	3.0694	3.6521	3.8385
α	3.8640	3.8012	3.6513	3.7905	3.3978	3.1295
β	-1.2880	-1.2496	-1.0715	-1.3753	-1.2082	-1.1896
γ	0.3268	0.3423	0.3109	0.3325	0.3348	0.4059
a	0.0000	0.0001	0.0002	0.0001	0.0000	-0.0001
b	-0.0711	-0.0847	-0.0916	-0.0858	-0.0629	-0.0557
c	4.8940	5.6105	5.6745	5.6113	4.6258	4.2271
S_e/S_y	0.0519	0.0579	0.1134	0.0519	0.0722	0.0867
R^2	0.9980	0.9975	0.9902	0.9980	0.9960	0.9943

5.2.1 Master curves generated using dynamic modulus results for all mixtures

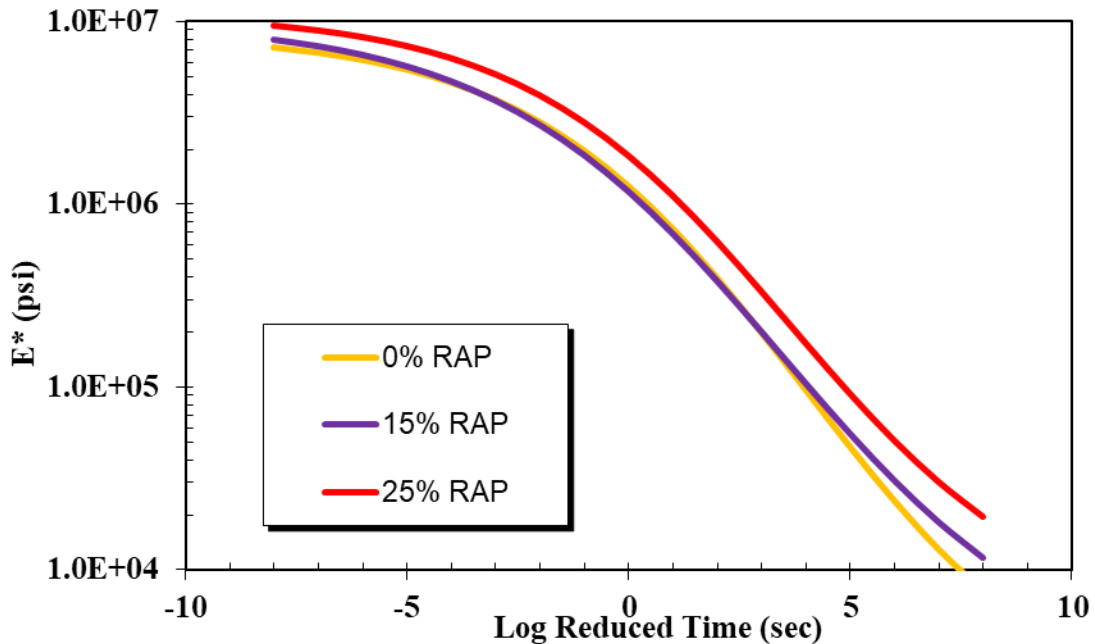


Figure 5.2 Master curve comparison of all RAP mixes

Figure 5.2 shows the comparison of the master curves for the 0%, 15% and 25% RAP mixes. It can be observed that the 0% and 15% RAP mixes showed almost similar stiffness except at higher temperatures where the 15% RAP mix showed stiffer behavior

than the 0% RAP mix. The 25% RAP mix showed stiffer behavior compared to other two mixes as expected due to the stiffening effect caused by the RAP.

Figure 5.3, Figure 5.4, Figure 5.5 show the master curves results for the OS mixes. It is observed that the mixes with OS showed softer behavior, at the extreme temperatures when compared to normal mixes. While the high temperature behavior needs further evaluation, the lower moduli at lower temperatures are actually desirable to reduce the potential for cracking, especially those reported for RAP mixtures. Figure 5.6 shows the comparison of Master curves for all six mixes.

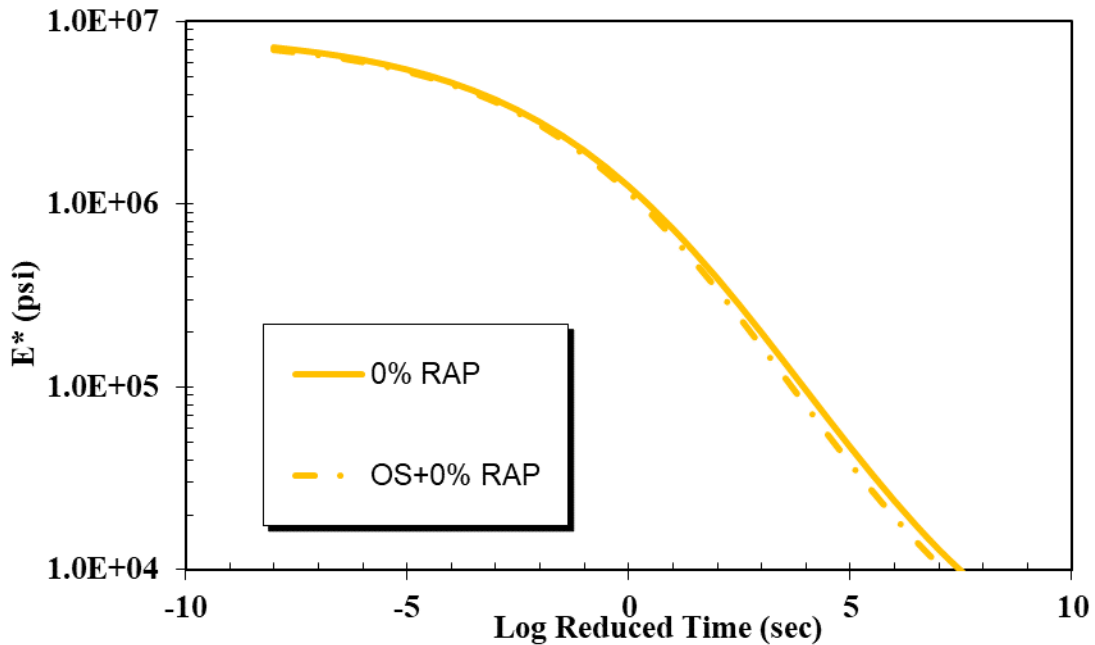


Figure 5.3 Master curve comparison between 0% RAP mixes with and without OS

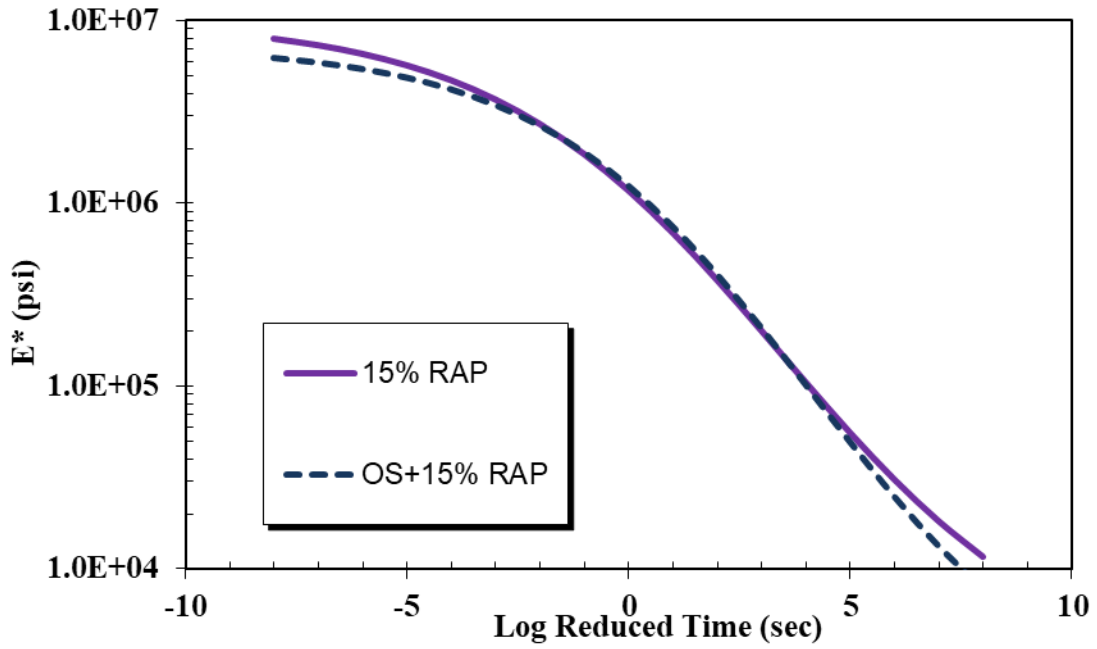


Figure 5.4 Master curve comparison for 15% RAP mixes with and without OS

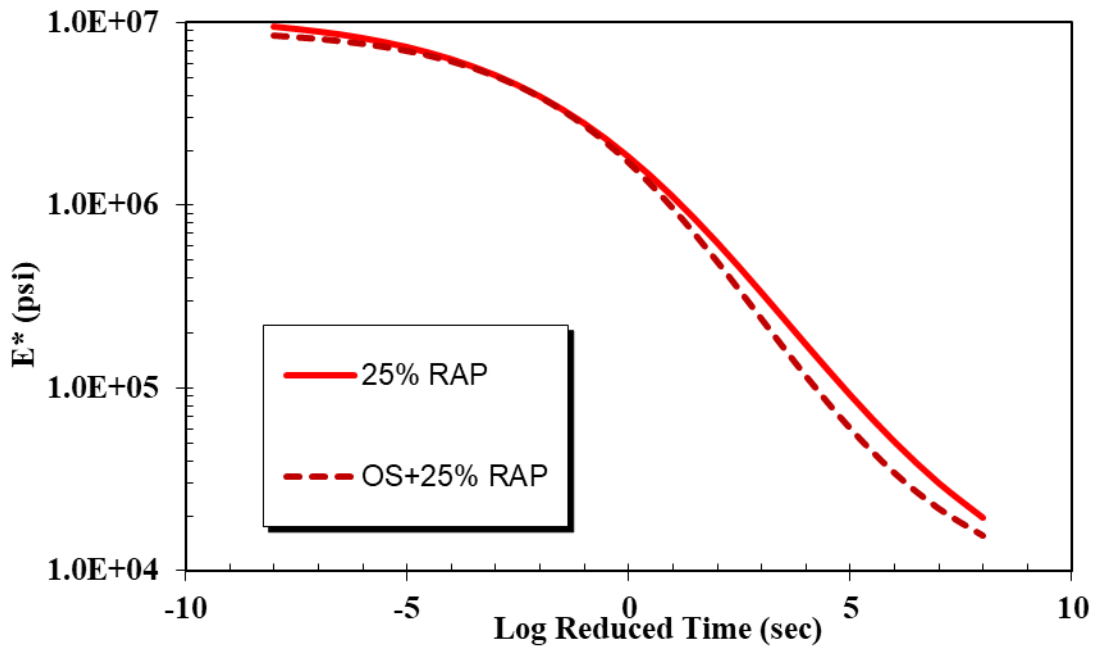


Figure 5.5 Master curve comparison for 25% RAP mixes with and without OS

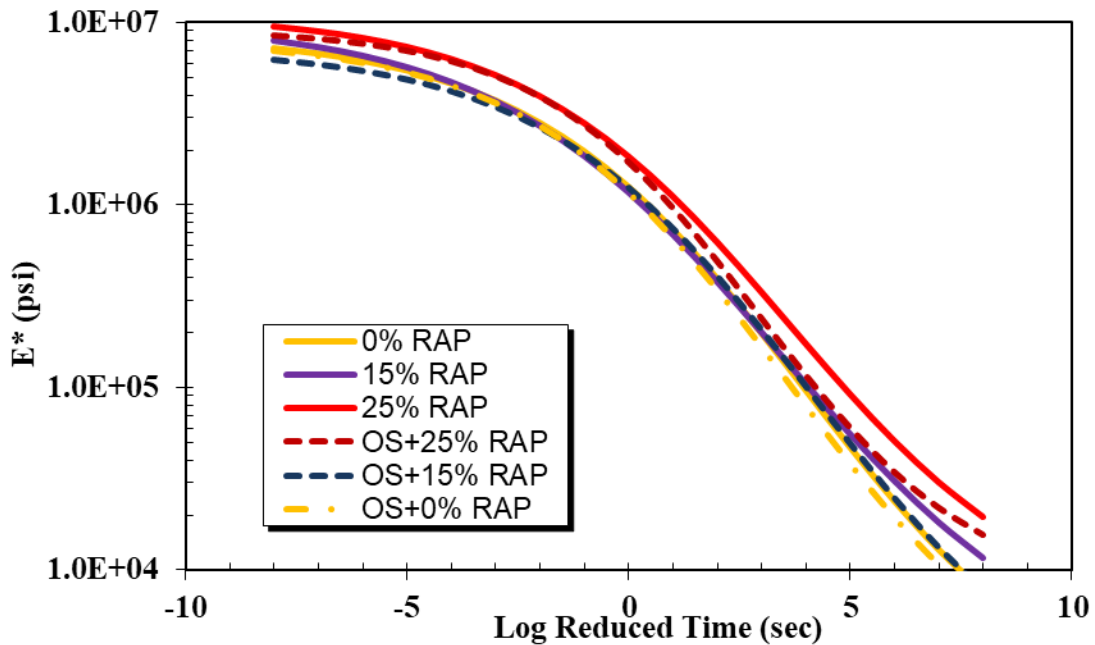


Figure 5.6 Master curve comparison for all the mixes

The OS+25% RAP mixture performance is favorable at the high temperature end (lower E^*); the OS+15% RAP mixture performance is also best at the low temperature end (high E^*) and comparable to the 0% RAP mixture performance at the high temperature end. These tentative results are promising in terms how OS can add further benefit to the use of the RAP mixture without risking pavement performance due to cracking or rutting.

5.2.2 Comparison of Modulus values of all mixtures at all frequencies for each temperature

To better demonstrate trends observed in the previous section, the modulus values obtained from the dynamic modulus test were also directly compared for each mix. The modulus values were plotted as histograms for each frequency. These plots for each

temperature are shown in Figure 5.7, Figure 5.8, Figure 5.9, Figure 5.10, Figure 5.11.

These plots also show that OS can reduce the additional stiffening behavior of the asphalt mixtures, especially at higher moduli values. RAP mixtures are typically prone for cracking and the OS may provide a mitigation for this development.

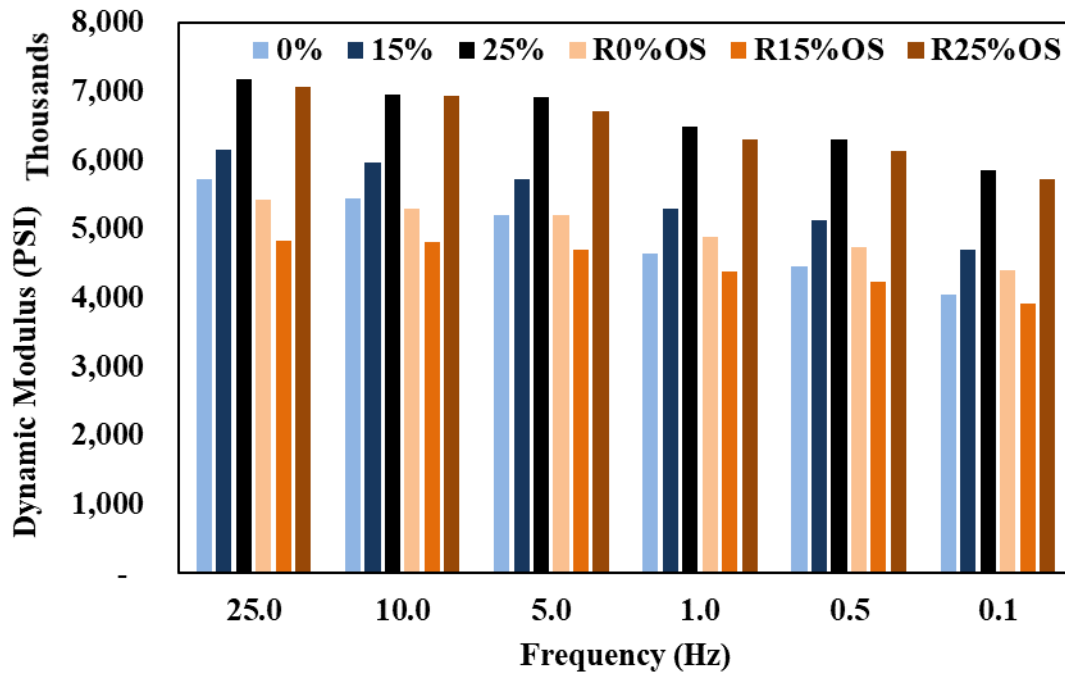


Figure 5.7 Modulus comparison of all mixtures at all frequencies at -10C

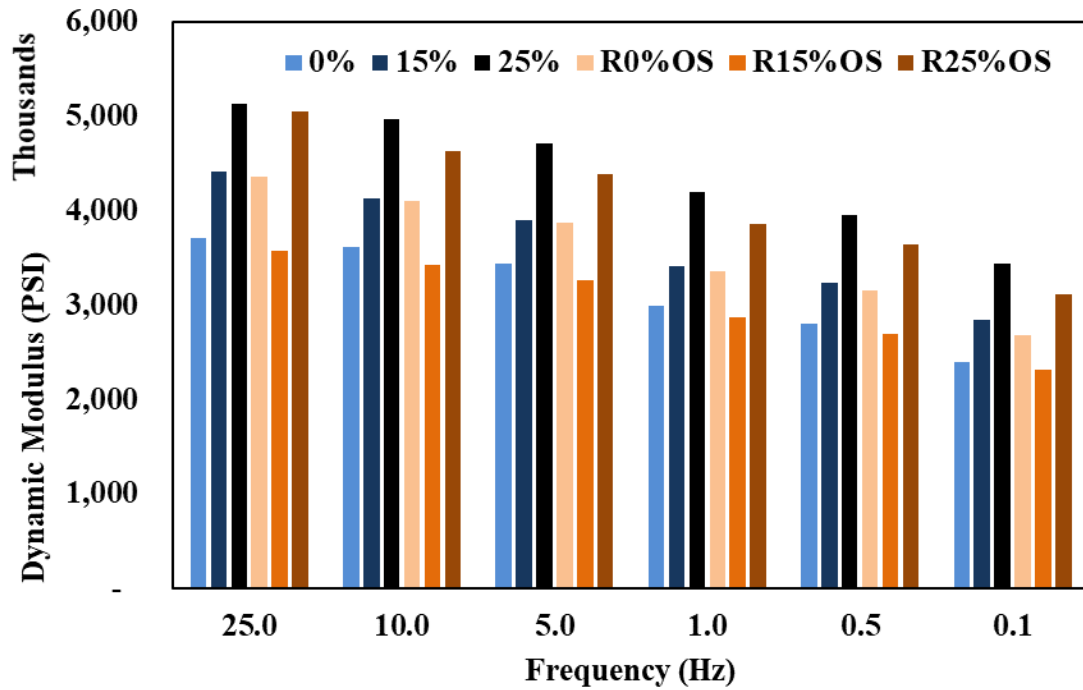


Figure 5.8 Modulus comparison of all mixtures at all frequencies at 4.4 C

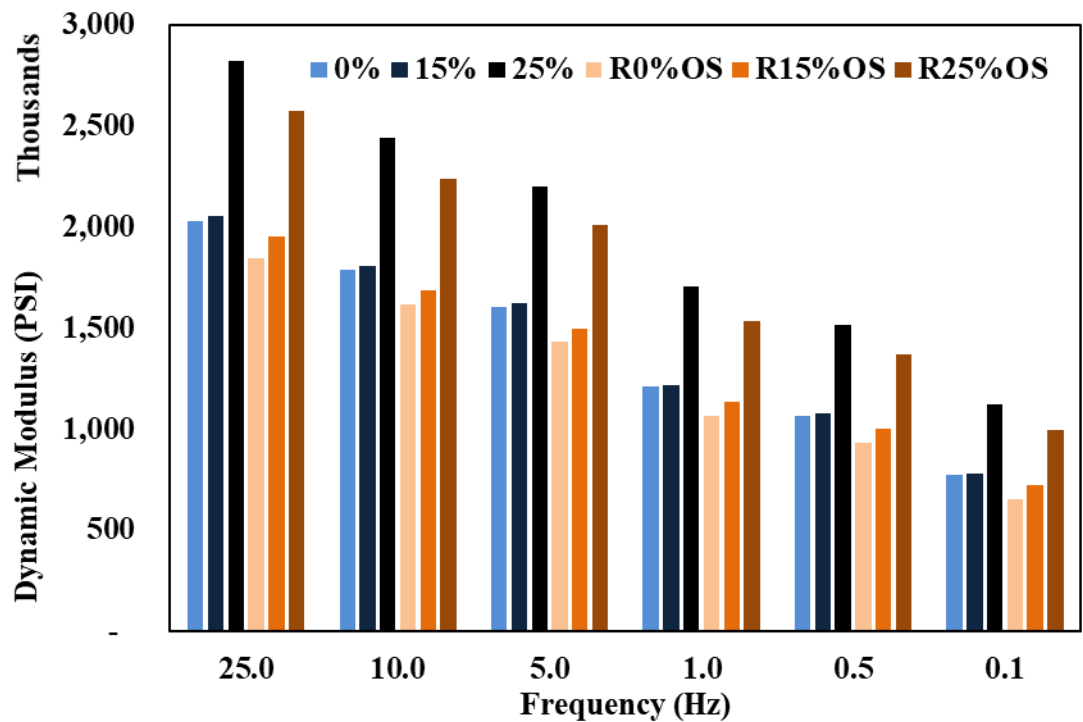


Figure 5.9 Modulus comparison of all mixtures at all frequencies at 21.1C

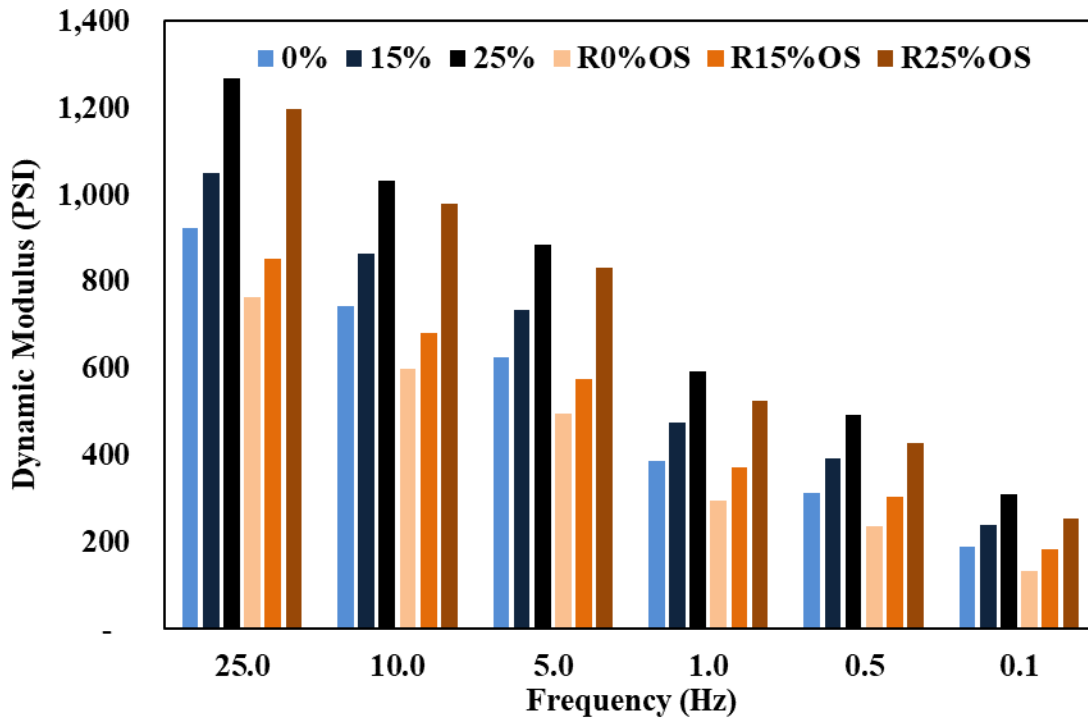


Figure 5.10 Modulus comparison for all mixtures at all frequencies at 37.8C

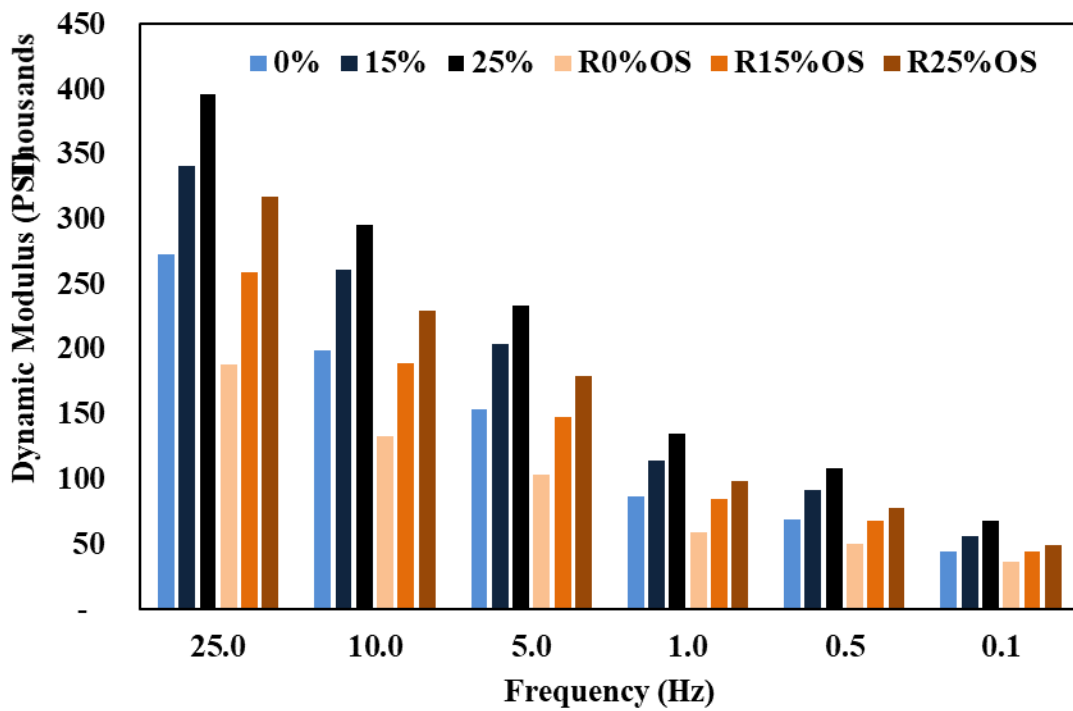


Figure 5.11 Modulus comparison for all mixtures at all frequencies at 54.4 C

5.3 Flow Number

Flow Number (FN) test was conducted by following the AASHTO TP-79 as discussed in Chapter 4. The test was conducted at a temperature of 50°C with an axial stress of 400 kPa. The FN was determined using Franken model approach. The FN results along with other parameters are shown in Table 5.7. The FN values are also compared for all six mixes in Figure 5.12. Detailed results and plots for flow number values were shown in APPENDIX C.

The resilient modulus results are consistent with the dynamic modulus results. That is, the OS results in reduced values at this test temperature of 50°C (except for the 25%RAP mix).

Table 5.7 Flow Number (FN) values for all six mixes

	FN	Resilient Modulus (psi)	Axial Permanent strain at failure ep (%)
0% RAP	1452	122768	1.347
0% RAP+OS	455	97349	1.603
15% RAP	2106	121045	1.43
15%RAP+OS	754	106219	1.355
25%RAP	5754	149125	1.233
25%RAP+OS	4090	165503	0.911

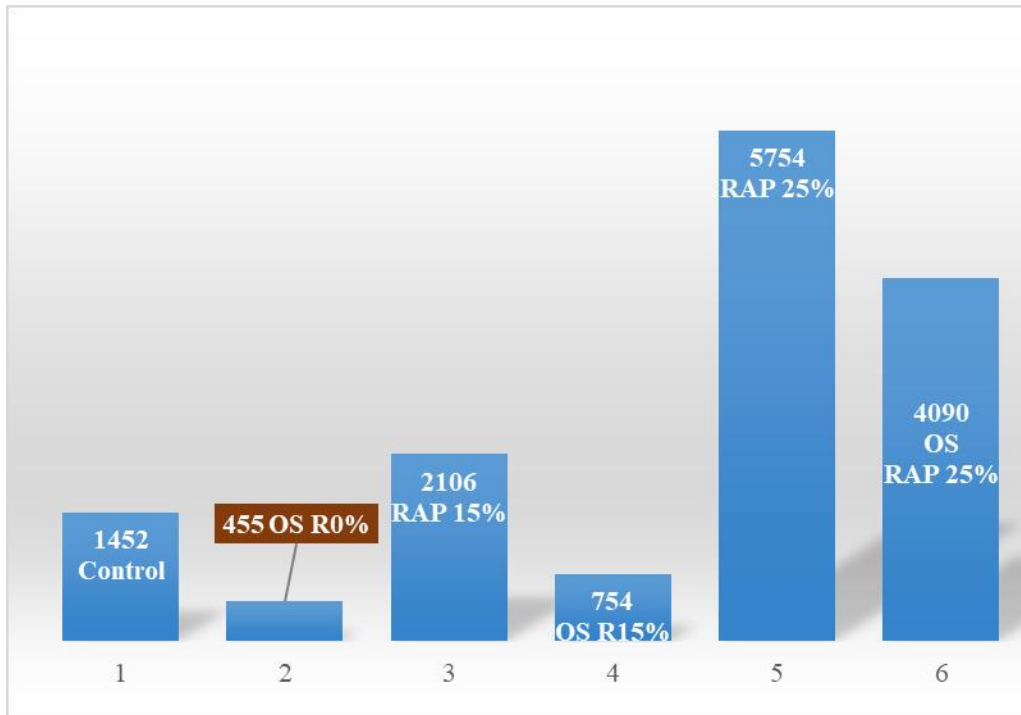


Figure 5.12 Comparison of flow number values for all six mixes

As shown in the figure, the FN increased with an increase in RAP content as expected. This is due to the increase in stiffness created by the RAP. By the addition of OS to mix, the flow number of the mix decreases. This decrease could be also due to reduced mixing and compaction temperatures, which would typically make the mix less stiff than those compacted at higher temperatures. The RAP 25% mix shows the highest values of flow number in all six mixes followed by 25% RAP + OS mix. The coefficient of variation between replicates of flow number samples were shown in APPENDIX C and the values were below 193% which is specified in AASHTO TP-79.

The rut depths for all the mixes were predicted by using the rutting prediction model presented in Chapter 4. For this prediction model, thickness of asphalt layer was assumed to be 3 inches and was measured at different ESAL's. The performance period is 20 years. The results are shown in Table 5.8. The results are favorable for mixtures

with 25%RAP with and without OS. However, the OS addition also provides lower cracking advantages as discussed in the previous section.

Table 5.8 Rut depth (in) calculated for 3 in thick layer for different ESALs

		ESAL's		
	FN	1.00E+07	3.00E+07	5.00E+07
0% RAP	1452	0.26	0.29	0.57
0% RAP+OS	455	0.35	0.39	0.76
15% RAP	2106	0.24	0.27	0.52
15%RAP+OS	754	0.31	0.34	0.67
25%RAP	5754	0.19	0.21	0.41
25%RAP+OS	4090	0.20	0.23	0.44

The FN values were calculated at an axial stress of 600 kPa using the flow number prediction model presented in Chapter 4. The values are compared to the measured values at 400kPa and shown in Table 5.9. The FN values at an axial stress of 600 kPa are also compared with the limits given in AASHTO TP 79 in

Table **5.10**. From these tables, the mixtures without OS have flow number value greater than the minimum average flow number required for HMA mixes for all the traffic levels. All the mixtures with OS except the control mix have flow number greater than the specification value for WMA mixes at all traffic levels. The flow number value for control mix with OS is less the specification value for WMA mix at traffic >30 million ESAL's but it is greater than the values at other traffic levels.

Table 5.9 Flow number values at different stress levels calculated using flow number prediction equation

Mixture	FN at axial stress 400 kPa	FN at axial stress 600 kPa
0% RAP	1452	1080
0% RAP+ OS	455	338
15% RAP	2106	1566
15% RAP+OS	754	561
25% RAP	5754	4280
25% RAP+OS	4090	3042

Table 5.10 Minimum Average flow number values for different traffic levels (AASHTO-TP79-15, 2016)

Traffic level, million ESALs	HMA Minimum Average Flow Number	WMA Minimum Average Flow Number
<3	-	-
3 to <10	50	30
10 to <30	190	105
>30	740	415

5.4 Tensile strength Ratio

The tensile strength ratio test was conducted by following AASHTO T 283 described in Chapter 4. The load was applied on the test samples at a rate of 50 mm/min. The results for all the mixes are shown in Table 5.11, Table 5.12, Table 5.13, Table 5.14, Table 5.15, and Table 5.16. The tables also give information about the average air voids of the subset, tensile strength of each specimen and tensile strength ratio of mix. Step by step calculations involved in calculating tensile strength ratio for all the mixes were shown in APPENDIX D.

Table 5.11 Tensile Strength Ratio results for Control mix

	Conditioned			Dry (Unconditioned)		
Average air voids	6.326			6.289		
Tensile strength (kPa)	1219.69	1286.26	1274.44	1561.13	1516.03	1437.34
Average tensile strength (kPa)	1260.13			1504.83		
Tensile Strength Ratio (%)	83.74					

Table 5.12 Tensile Strength Ratio test results for 0% RAP mix with OS

	Conditioned			Dry (Unconditioned)		
Average air voids	6.008			6.084		
Tensile strength (kPa)	1672.02	1543.23	1555.60	1862.87	1958.10	1662.80
Average tensile strength (kPa)	1590.29			1827.93		
Tensile Strength Ratio	87.00					

Table 5.13 Tensile Strength Ratio test results of 15% RAP mix

	Conditioned			Dry (Unconditioned)		
Average air voids	6.412			6.485		
Tensile strength (kPa)	1506.73	1279.06	1496.29	1495.68	1680.83	1664.70
Average tensile strength (kPa)	1427.36			1613.74		
Tensile Strength Ratio	88.45					

Table 5.14 Tensile Strength Ratio test results for 15% RAP mix with OS

	Conditioned			Dry (Unconditioned)		
Average air voids	6.326					
Tensile strength (kPa)	1806.33	1794.50	1719.24	1877.01	2034.24	2001.96
Average tensile strength (kPa)	1773.35			1971.07		
Tensile Strength Ratio	89.97					

Table 5.15 Tensile Strength Ratio test results for 25% RAP mix

	Conditioned			Dry (Unconditioned)		
Average air voids	6.194			6.171		
Tensile strength (kPa)	1851.60	1805.36	2081.75	2059.03	1929.19	2271.14
Average tensile strength (kPa)	1912.90			2086.45		
Tensile Strength Ratio	91.68					

Table 5.16 Tensile Strength Ratio test results 25% RAP mix with OS

	Conditioned			Dry (Unconditioned)		
Average air voids	5.93			5.941		
Tensile strength (kPa)	2225.92	2279.35	2318.98	2294.08	2423.21	2433.35
Average tensile strength (kPa)	2274.75			2383.54		
Tensile Strength Ratio	95.44					

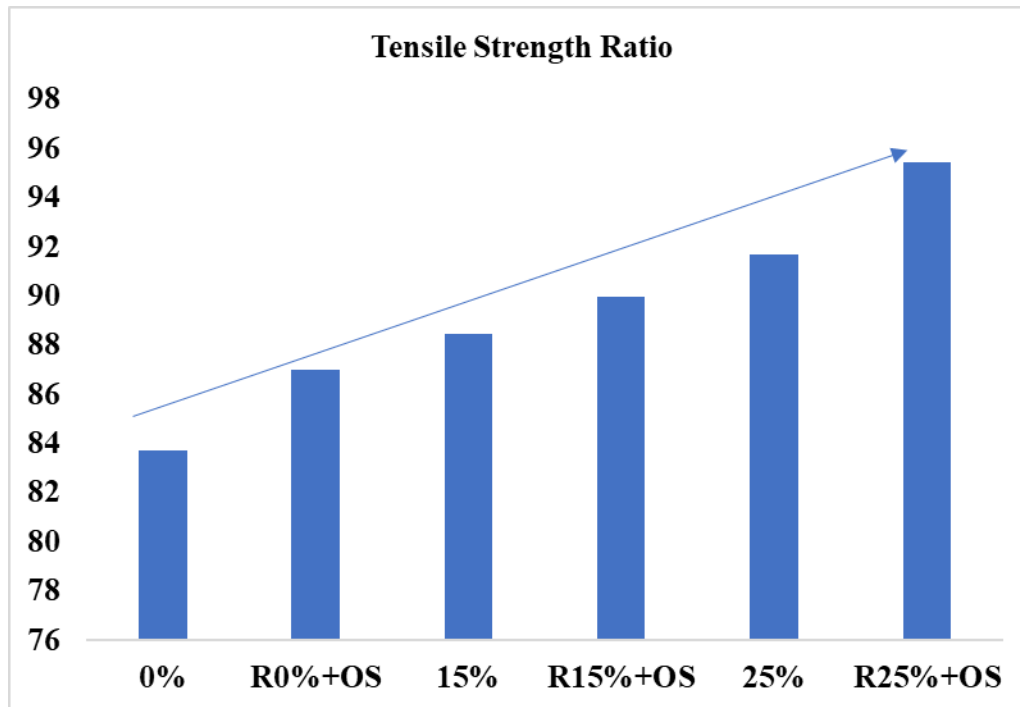


Figure 5.13 Comparison plot for TSR values of all mixes

The tensile strength ratio results are also plotted for all six mixes as shown in Figure 5.13. From this plot, it can be observed that the TSR increases with increase in

RAP, which is expected because the presence of old stiff binder restricts stripping of the binder. Mixes with OS also showed improved moisture resistance. In reality, the reduction in compaction temperatures should make the mixtures more susceptible to moisture; however, it is true that the declared benefit of adding OS would result in an increase in bonding between the aggregate and binder. The moisture resistance of the OS mixes increased. All of these results are compared in Table 5.17 for the direct comparison. The mixtures with OS also showed higher strength values in both the conditioned and unconditioned subsets.

Table 5.17 Comparison of TSR values of all mixes

Mix	Dry Strength(kPa)	Wet Strength (kPa)	TSR (%)
0% RAP	1504.8	1260.1	84
0 % RAP + OS	1828	1590	87
15% RAP	1613.7	1427.4	88
15 % RAP + OS	1971	1773	90
25% RAP	2086	1913	92
25 % RAP + OS	2384	2275	95

Chapter 6 Summary, Conclusions and Recommendations

6.1 Summary

Use of Recycled Asphalt Pavement (RAP) in newly designed asphalt mixtures is becoming a common practice in the recent past, especially to be conscious of diminishing non-renewable resources like aggregates and asphalt binders. Depending on the percentage of RAP, the stiffness of the hot mix asphalt (HMA) increases by including RAP in mixes. In a climatic area such as the City of Phoenix, RAP properties are expected to be more oxidized and aged compared to other regions across the US. Therefore, there are concerns about the cracking behavior and long-term performance of asphalt mixes with high percentage of RAP.

Another problem facing the asphalt pavement industry is stripping or moisture damage. Even in Arizona that do not see heavy rain throughout the year, there are time periods (such as the monsoon season) where we have seen asphalt pavements fail by stripping. One product of interest in this study was the Organosilane (OS), which has the potential to improve the bond between the aggregate and asphalt binder, as it modifies the aggregate structure from hydrophilic to hydrophobic state. This improves the moisture resistance of the asphalt mixture. The use of Organosilane also reduces the mixing and compaction temperatures required for asphalt mixtures, and indirectly makes the asphalt mixture production process as a Warm Mix Asphalt technology. The use of Organosilane in this study was also hypothesized to reduce the additional stiffening behavior that may result from the use of RAP in the Phoenix area; and therefore, reduce the additional cracking potential of the asphalt mixtures when using RAP.

In this study, six asphalt mixes were prepared with three RAP contents, 0% (control), 15% and 25%, with and without Organosilane. The dosage of Organosilane used was 0.08% for 0% and 15% RAP contents, and 0.088% for the 25% RAP mixture. In addition, when the Organosilane was used, the mixing temperature was reduced by 10°C and the compaction temperature was reduced by 30°C. Mix designs were performed, and the volumetric properties were compared. The mixture laboratory performance was evaluated for all mixture by conducting Dynamic Modulus, Flow Number and Tensile Strength Ratio tests.

6.2 Conclusions

The findings from the study were as follows:

- As the percentage of RAP increased, the optimum amount of virgin binder decreased to achieve the 4% air voids. The optimum binder contents were 5.02%, 5.37% and 5.75% for 0%, 15% and 25% RAP mixes, respectively. The virgin binder added to the 15% and 25% RAP mixes was 4.8% and the balance was contributed from the RAP material.
- When the binder was modified with Organosilane, all mixtures achieved better compaction at a reduced temperature of 30°C.
- The dynamic modulus results showed similar values for mixtures with 0% and 15% RAP; however, stiffness was increased for the 25% RAP mix.
- Mixtures modified with Organosilane generally exhibited softer behavior at the extreme ends of lower and higher temperatures. While the high temperature behavior needs to be carefully considered in terms of the RAP percentage, the

- lower moduli at lower temperatures are actually desirable to reduce the potential for cracking. One reason for these lower stiffness is due to reduction in the mix compaction temperatures, making it similar to a Warm Mix Asphalt (WMA).
- For the Flow Number (FN) test, as RAP content increased, the FN values also increased showing the potential increase in rutting resistance.
 - When the Organosilane was used, the FN values decreased mainly due to the softer behavior of the mixtures. The results were favorable for the 25% RAP mix with and without OS. Keeping in mind that the OS addition also provides lower cracking advantages as demonstrated by the dynamic modulus tests.
 - The FN values for the RAP mixtures with OS also passed the minimum required at all traffic levels given in AASHTO TP 79.
 - Tensile Strength Ratio (TSR) results increased with the increase in RAP percentage, and further increase was observed when OS was used.
 - In reality, the reduction in compaction temperatures should make the mixtures more susceptible to moisture; however, the OS resulted in an increase in bonding between the aggregate and binder.
 - The mixtures with OS also showed higher strength values in both the conditioned and unconditioned subsets.
 - The Organosilane reduced the sticking nature of the binder to the metal molds and equipment, which reduced the efforts in cleaning them. As reduced temperatures were used in preparing these mixes, it also saves energy and better compaction was achieved.

- Based on the experiments in this study, the use of RAP saves non-renewable resources and contributes to the sustainability benefits of pavements.
- The use of Organosilane may facilitates higher percentage of RAP usage as it reduces the stiffening behavior of the asphalt mix ; The Organosilane improves the moisture resistance of asphalt mixtures, especially when lower compaction temperatures are used.

6.3 Recommendations for Future Work

- The current study was limited to three basic performance tests and moderate RAP percentages. Future studies should consider additional performance tests such as fatigue and crack propagation (C* Fracture Test); and higher percentages of RAP.
- The characteristics of Organosilane modified binders need to be studied to better understand binder properties, and changes in performance grade and/or aging conditions.
- The dosage of Organosilane used was 0.088%; future research can explore an increased value or finding an optimum percentage for modification. Would it be also affected by the PG binder grade?
- Using other moisture damage assessment may be of interest, such as using the blister test and/or the ESR (E* Strength Ratio).

REFERENCES

- AASHTO-T166. (2016). *Standard Method of Test for Bulk Specific Gravity (Gmb) of Compacted Hot Mix Asphalt (HMA) Using Saturated Surface-Dry Specimens*. Washington, D.C: American Association of State Highway and Transportation Officials.
- AASHTO-T209. (2016). *Standard Method of Test for Theoretical Maximum Specific Gravity (Gmm) and Density of Hot Mix Asphalt (HMA)*. Washington, D.C: American Association of State Highway and Transportation Officials.
- AASHTO-T283. (2016). *Standard Method of Test for Resistance of Compacted Asphalt Mixtures to Moisture Induced Damage*. Washington D.C: American Association of State Highway and Transportation Officials.
- AASHTO-T342. (2011). *Standard Method of Test for Determining Dynamic Modulus of Hot Mix Asphalt (HMA)*. Washington, D.C: American Association of State Highway and Transportation Officials.
- AASHTO-TP79-15. (2016). *Standard Method of Test for Determining the Dynamic Modulus and Flow Number for Asphalt Mixtures Using the Asphalt Mixture Performance Tester (AMPT)*. Washington, D.C: American Association of State Highway and Transportation Officials.
- Abbas Booshehrian, W. S. (2013). How to construct an Asphalt Binder Master curve and Assess the Degree of Blending between RAP and Virgin Binders. *Journal of Materials in Civil Engineering*.
- Ahmed Mohamady, A. E. (2014). Effect of Using Reclaimed Asphalt Pavement on Asphalt Mix Performance. *IOAR Journal of Computer Engineering*, 55-67.
- Ajay Ranka, P. M. (2014). Nanotechnology Organosilane Compounds for Chemical Bonding in Road Construction. *Asphalt Pavement Technology*, 703-716.
- Anderson, E. D. (2012). *Long Term Performance of High RAP Pavements: Case Studies*. Durham, NH: University of New Hampshire.
- Arianna Stimilli, A. V. (2017). *Mix design Validation through performance-related analysis of in plant asphalt mixtures containing high RAP content*. *International Journal of Pavement Research and Technology*.
- Arif Chowdhury, J. W. (2008). *A Review of Warm Mix Asphalt*. College Station, TX: Texas Transportation Institute.
- Bonaquist, R. (2012). *Evaluation of Flow number as a discriminating HMA mixture Property*. Madison, WI: Wisconsin Department of Transportation.
- Copeland, A. (2011). *Reclaimed Asphalt Pavement in Asphalt Mixtures: State of Practice*. McLean, VA: Federal Highway Administration .

- Fujie Zhou, S. H. (2014). *Balanced RAP/RAS Mix Design System for Project-Specific Conditions*. Texas A&M Transportation Institute, Texas Department of Transportation. Lancaster, Pennsylvania: Asphalt Paving Technology.
- Gonzalo Arredondo, S. G. (2017). *Reclaimed Asphalt Pavement Project; Phase-1*. Phoenix: City of Phoenix.
- HMA Mix Design Fundamentals*. (2012). Retrieved 03 04, 2018, from Pavement interactive: <http://www.pavementinteractive.org/hma-mix-design-fundamentals/>
- Imad L. Al-Qadi, Q. A. (2012). *Impact of High RAP Contents on Structural and Performance Properties of Asphalt Mixtures*. Urbana, Illinois: University of Illinois at Urbana-Champaign.
- Jo Sias Daniel, A. L. (2005). *Mechanistic and Volumetric Properties of Asphalt mixtuers with RAP*. Durham, NH: University of New Hampsire.
- Kiggundu, R. (1988). *Stripping in HMA Mixtures: State of the Art and Critical Reviews of Test Methods*. Auburn, AL: National Center for Asphalt Technology.
- M.Z. Alavi, Y. J. (2015). *Evaluation of the Combined Effects of Reclaimed Asphalt Pavement (RAP), Reclaimed Asphalt Shingles (RAS), and Different Virgin Binder Sources on the Performance of Blended binders for Mixes with Higher Percentages of RAP and RAS*. Berkly, California: National Center for Sustainable Transportation.
- Maria C. Rodezno, K. E. (2013). DEvelopment and Validation of a Rutting Model for Asphalt Mixtures Based on the Flow Number Test. *Asphalt Pavement Technology*, 82, 557-578.
- Mirzababaei, P. (2016). Effect of zycotherm on moisture susceptibility of Warm Mix Asphalt mixtures prepared with different aggregate types and gradations. *Construction and Building Materials* , 116.
- Mohamad Javad Ayazi, A. M. (2017). Moisture Susceptibility of warm mixed-reclaimed asphalt pavement containing Sasobit and Zycotherm additives. *Petroleum Science and Technology*, 35(9).
- Mohd Rosli Mohd Hasan, M. O. (2017). Performance characterization of asphalt binders and mxtures incorporating silane additive Zycotherm. *AIP Conference Proceedings*, 1892(1).
- Moisture Susceptibility*. (2012). Retrieved 3 7, 2018, from Pavement interactive: <http://www.pavementinteractive.org/moisture-susceptibility/>
- Phoenix, C. o. (2015). *City of Phoenix supplement to the 2015 Edition Maricopa Association of Governments Uniform Standard Specifications for Public Works Construction*. Phoenix: City of Phoenix.

- Randy West, J. R. (2013). *NCHRP Report 752: Improved Mix Design, Evaluation, and Materials Management Practices for Hot Mix Asphalt with High Reclaimed Asphalt Pavement Content*. Washington D.C: Transportation Research Board.
- Ranka, A. (2018, April 18). Interaction of Organosilane with binder. (K. Kaloush, P. Kaligotla, & G. Arredondo, Interviewers)
- Ranka, D. A. (2014). Organo-Silane Nanotechnologies Additives for " Moisture Resistant Asphalt Roads". *AAPT- International Forum*. Atlanta-GA.
- Raveesh J, M. S. (2017). Laboratory Evaluation of WMA with Zycotherm Warm Mix Additive. *International Journal for Research in Applied Science & Engineering Technology*, 5(7).
- Rebecca McDaniel, M. A. (2001). *NCHRP Report 452: Recommended Use of Reclaimed Asphalt Pavement in the Superpave Mix Design Method: Technicians Manual*. Washington, D.C-2001: Transportation Research Board- National Research Council.
- Rodezno M.C, K. K. (2010). Development of Flow Number Predictive Model. *Transportation Research Record*, 79-87.
- Rohith N, J. R. (2013). A Study on Marshall Stability Properties of Warm Mix Asphalt Using Zycotherm A Chemical Additive. *International Journal of Engineering Research & Technology*, 2(7).
- West, R. C. (2010). *Reclaimed Asphalt Pavement Management*. Auburn: National Center for Asphalt Technology (NCAT).
- Witczak M.W, K. K.-B. (2002). *Simple Performance Test for Superpave Mix Design: NCHRP Report 465*. Tempe: National Academy Press.
- Y. Richard Kim, B. U. (2011). *LTPP Computed Parameter: Dynamic Modulus*. McLean, VA: Federal Highway Administration.
- Zaniewski J, a. V. (2006). *Investigation of Moisture Sensitivity of Hot Mix Asphalt*. University of West Virginia, Dept. of Civil & Environmental Engineering . Morgantown, WV: Asphalt Technical Program.
- Zaumanis, M. (2010). *Warm Mix Asphalt Investigation*. Denmark: Technical University of Denmark.
- Zydex. (2014). *Zycotherm-SP Lab Protocol*. Vadodara, India: Zydex Industries.
- Zydexindustries. (2015, September 19). *Road Solutions*. Retrieved 2018, from Zydex Industries: <http://www.zydexindustries.com/roads-products.aspx?key=uORpM5MhoHF4EE/oKvePiw==>

APPENDIX A
MIX DESIGN CALCULATIONS

0% RAP mix

G_{mb} calculations for 0% RAP mix

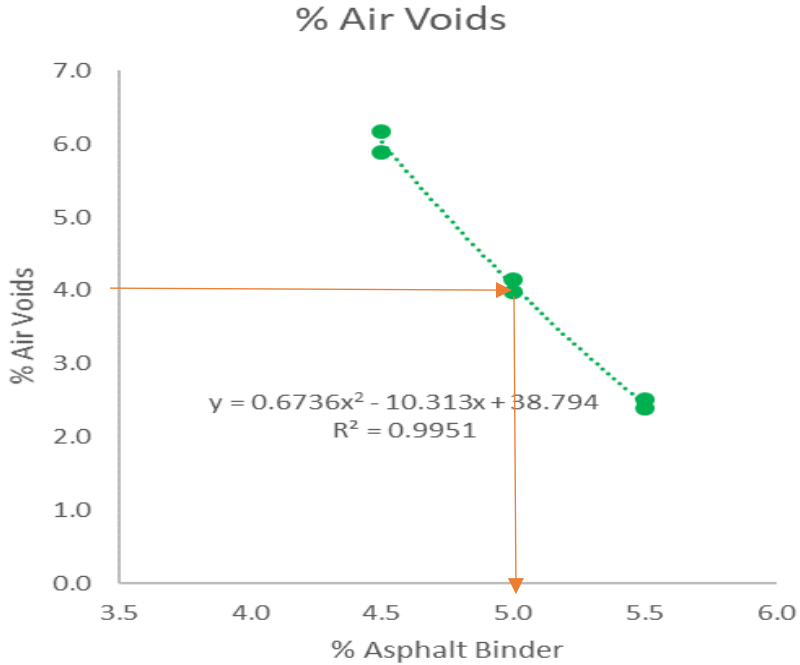
Binder Percentage	Gmm	Mass in air (A) gm	Mass SSD (C) gm	Mass in water (B) gm	Sample Vol (C-B) gm	Gmb A/(C-B)	% Air voids (1-Gmb/Gmm)*100
4.50%	2.477	4689.1	4703.9	2705.8	1998.1	2.347	5.2
4.50%	2.477	4693.4	4710.5	2718.8	1991.7	2.356	4.9
5%	2.458	4691.3	4695.5	2725.1	1970.4	2.381	3.1
5%	2.458	4689.4	4695.2	2729.2	1966	2.385	3.0
5.50%	2.440	4688.8	4692.3	2741.5	1950.8	2.404	1.5
5.50%	2.440	4689.8	4691.5	2743.1	1948.4	2.407	1.4

Calculating correction factor from measured and estimated values of G_{mb}

Pb	Mass gm	Volume at different heights (Cu.cm)			Gmb (estimated)			Gmb (measured)	Correction factor
		N ini	N des	N max	ini	Des	max		
4.5	4691.0	2189.5	2041.6	2021.6	2.143	2.298	2.320	2.347	1.011
4.5	4694.0	2206.8	2041.9	2019.8	2.127	2.299	2.324	2.356	1.014
5.0	4692.0	2165.6	2017.6	1996.5	2.167	2.326	2.350	2.381	1.013
5.0	4691.0	2160.2	2011.5	1990.5	2.172	2.332	2.357	2.385	1.012
6	4691	2148	1998	1978	2.184	2.348	2.372	2.404	1.01
6	4691	2133.7	1987	1966	2.199	2.361	2.386	2.407	1.01

Calculations for design air voids for all the replicates to find out the optimum binder content

Gmb corrected			Gmm	%Gmm			% Air voids
N ini	N des	N max		N ini	N des	N max	@Ndes
2.167	2.324	2.347	2.477	87.5	93.8	94.8	6.2
2.157	2.331	2.356	2.477	87.1	94.1	95.1	5.9
2.195	2.356	2.381	2.458	89.3	95.8	96.9	4.2
2.198	2.360	2.385	2.458	89.4	96.0	97.0	4.0
2.213	2.379	2.404	2.440	90.7	97.5	98.5	2.5
2.218	2.382	2.407	2.440	90.9	97.6	98.6	2.4



Plot between the air void percentage and binder content to find OBC

15% RAP Mix

G_{mb} calculations for 15% RAP mix

Sample	G _m	Mass in air (A) (gm)	Mass SSD (C) (gm)	Mass in water (B) (gm)	Sample Vol (C-B) (gm)	G _{mb} A/(C-B)	% Air voids (1-G _{mb} /G _{mm})*100
4.50%	2.521	4913.4	4916.2	2888.8	2027.4	2.423	3.8
4.50%	2.506	4937	4940.7	2913.8	2026.9	2.436	2.8
5.00%	2.509	4953.9	4955.4	2921	2034.4	2.435	2.9
5.00%	2.498	4941	4942.2	2911.2	2031	2.433	2.6
5.50%	2.471	4955.3	4956.8	2917.8	2039	2.430	1.7
5.50%	2.458	4956.6	4957.4	2916.9	2040.5	2.429	1.2

Calculations for design air voids for all the replicates to find out the optimum binder content

G _{mb} corrected			G _{mm}	%G _{mm}			% Air voids @N _{des}
N _{ini}	N _{des}	N _{max}		N _{ini}	N _{des}	N _{max}	
2.227	2.400	2.423	2.521	88.4	95.2	96.2	4.8
2.248	2.413	2.436	2.506	89.7	96.3	97.2	3.7
2.251	2.412	2.435	2.509	89.7	96.1	97.1	3.9
2.240	2.410	2.433	2.498	89.6	96.5	97.4	3.5
2.249	2.412	2.430	2.471	91.0	97.6	98.3	2.4
2.252	2.410	2.429	2.458	91.6	98.0	98.8	2.0

25% RAP Mix

G_{mb} calculations for 25% RAP mix

Binder content	G _{mm}	Mass in air (A) (gm)	Mass SSD (C)(gm)	Mass in water (B)(gm)	Sample Vol (C-B) (gm)	G _{mb} A/(C-B)	% Air voids (1-G _{mb} /G _{mm})*100
5%	2.506	4700.1	4716.3	2732.4	1983.9	2.369	5.4
5%	2.506	4700.6	4716.4	2737.1	1979.3	2.375	5.2
6%	2.479	4700.2	4708	2745	1963	2.394	3.4
6%	2.479	4699.1	4706.8	2749.3	1957.5	2.401	3.2
6%	2.467	4696.9	4701.5	2748.5	1953	2.405	2.5
6%	2.467	4698.9	4707.4	2748.6	1958.8	2.399	2.8

Calculations for design air voids for all the replicates to find out the optimum binder content

Gmb corrected			Gmm	%Gmm			% Air voids
N ini	N des	N max		N ini	N des	N max	@Ndes
2.158	2.343	2.369	2.506	86.1	93.5	94.6	6.5
2.152	2.349	2.375	2.506	85.9	93.7	94.8	6.3
2.175	2.369	2.394	2.479	87.8	95.6	96.6	4.4
2.181	2.375	2.401	2.479	88.0	95.8	96.8	4.2
2.177	2.380	2.405	2.467	88.2	96.5	97.5	3.5
2.174	2.375	2.399	2.467	88.1	96.3	97.2	3.7

APPENDIX B
DYNAMIC MODULUS RESULTS

Dynamic Modulus (ksi) values for all replicates for 0% RAP mix

Temp °C	Frequency Hz	0% RAP					
		3	7	9	AVG	std	cv%
10 °C	25	5859	7050	4248	5719	1148	20
10 °C	10	5717	6552	4081	5450	1026	19
10 °C	5	5498	6123	3978	5200	901	17
10 °C	1	5037	5230	3664	4644	697	15
10 °C	0.5	4845	5007	3536	4463	659	15
10 °C	0.1	4389	4524	3210	4041	590	15
4.4°C	25	2748	5304	3065	3705	1138	31
4.4 °C	10	2664	5211	2947	3608	1140	32
4.4°C	5	2539	4959	2814	3437	1082	31
4.4 °C	1	2213	4299	2443	2985	934	31
4.4°C	0.5	2075	4032	2306	2805	873	31
4.4 °C	0.1	1776	3443	1973	2397	744	31
21.1°C	25	1943	2101	2032	2025	65	3
21.1 °C	10	1730	1838	1788	1785	44	2
21.1°C	5	1560	1646	1609	1605	36	2
21.1 °C	1	1152	1248	1220	1207	40	3
21.1°C	0.5	1027	1086	1081	1064	27	3
21.1 °C	0.1	750	770	789	770	16	2
37.8°C	25	988	1074	708	923	156	17
37.8 °C	10	763	880	591	744	119	16
37.8°C	5	649	734	490	624	101	16
37.8 °C	1	395	447	317	386	54	14
37.8°C	0.5	322	359	256	312	43	14
37.8 °C	0.1	199	215	154	189	26	14
54.4°C	25	289	331	198	272	55	20
54.4 °C	10	214	243	139	199	44	22
54.4°C	5	165	185	112	154	31	20
54.4 °C	1	95	104	60	86	19	22
54.4°C	0.5	74	84	48	69	15	22
54.4 °C	0.1	47	56	30	44	11	24

Dynamic Modulus (ksi) values for all replicates for 0% RAP+OS mix

Temp °C	Frequency Hz	0% RAP + OS					
		3	7	9	AVG	std	cv%
10 °C	25	5265	5683	5346	5431	181	3
10 °C	10	5124	5523	5265	5304	165	3
10 °C	5	4985	5419	5182	5195	177	3
10 °C	1	4682	5187	4796	4888	216	4
10 °C	0.5	4525	5053	4642	4740	226	5
10 °C	0.1	4120	4689	4242	4350	245	6
4.4 °C	25	4664	4326	4068	4353	244	6
4.4 °C	10	4368	4057	3856	4094	210	5
4.4 °C	5	4116	3872	3633	3874	197	5
4.4 °C	1	3621	3333	3122	3359	205	6
4.4 °C	0.5	3406	3140	2924	3157	197	6
4.4 °C	0.1	2899	2689	2454	2681	182	7
21.1 °C	25	1647	1985	1905	1846	144	8
21.1 °C	10	1438	1737	1663	1613	127	8
21.1 °C	5	1285	1546	1470	1434	110	8
21.1 °C	1	957	1147	1078	1061	79	7
21.1 °C	0.5	831	1008	947	929	73	8
21.1 °C	0.1	586	718	655	653	54	8
37.8 °C	25	849	743	701	764	62	8
37.8 °C	10	659	593	542	598	48	8
37.8 °C	5	549	492	445	495	43	9
37.8 °C	1	328	300	261	296	27	9
37.8 °C	0.5	261	242	207	237	23	10
37.8 °C	0.1	153	135	113	134	16	12
54.4 °C	25	162	238	163	188	35	19
54.4 °C	10	120	166	114	133	23	18
54.4 °C	5	97	124	89	103	15	14
54.4 °C	1	62	68	49	59	8	13
54.4 °C	0.5	54	55	42	50	6	12
54.4 °C	0.1	40	37	31	36	4	11

Dynamic Modulus (ksi) values for all replicates for 15% RAP mix

Temp °C	Frequency Hz	15% RAP					
		3	7	9	AVG	std	cv%
10 °C	25	5831	5918	6705	6151	393	6
10 °C	10	5707	5859	6307	5958	255	4
10 °C	5	5543	5720	5928	5730	158	3
10 °C	1	5161	5339	5361	5287	89	2
10 °C	0.5	4985	5214	5154	5117	97	2
10 °C	0.1	4620	4806	4651	4692	82	2
4.4 °C	25	5198	4204	3827	4410	578	13
4.4 °C	10	4861	3846	3659	4122	528	13
4.4 °C	5	4586	3668	3429	3894	499	13
4.4 °C	1	4020	3268	2947	3412	450	13
4.4 °C	0.5	3800	3110	2786	3232	423	13
4.4 °C	0.1	3326	2728	2460	2838	362	13
21.1 °C	25	2218	2163	1784	2055	193	9
21.1 °C	10	1947	1898	1575	1807	165	9
21.1 °C	5	1717	1737	1418	1624	146	9
21.1 °C	1	1259	1332	1054	1215	118	10
21.1 °C	0.5	1101	1183	936	1073	103	10
21.1 °C	0.1	803	865	669	779	82	11
37.8 °C	25	1128	1060	959	1049	70	7
37.8 °C	10	930	871	791	864	57	7
37.8 °C	5	787	755	665	736	52	7
37.8 °C	1	518	494	415	476	44	9
37.8 °C	0.5	431	413	332	392	43	11
37.8 °C	0.1	266	250	197	238	29	12
54.4 °C	25	321	363	338	341	17	5
54.4 °C	10	240	271	272	261	15	6
54.4 °C	5	191	207	215	204	10	5
54.4 °C	1	109	113	121	115	5	4
54.4 °C	0.5	87	89	98	92	5	5
54.4 °C	0.1	55	51	62	56	5	8

Dynamic Modulus (ksi) values for all replicates for 15% RAP+OS mix

Temp °C	Frequency Hz	15% RAP + OS					
		3	7	9	AVG	std	cv%
10 °C	25	4613	4968	4921	4834	157	3
10 °C	10	4731	4901	4809	4814	70	1
10 °C	5	4624	4785	4689	4699	66	1
10 °C	1	4310	4419	4398	4376	47	1
10 °C	0.5	4172	4288	4240	4233	47	1
10 °C	0.1	3872	3953	3918	3914	33	1
4.4 °C	25	3587	3953	3178	3573	316	9
4.4 °C	10	3438	3688	3122	3416	232	7
4.4 °C	5	3276	3521	2985	3260	219	7
4.4 °C	1	2882	3083	2615	2860	191	7
4.4 °C	0.5	2727	2898	2466	2697	178	7
4.4 °C	0.1	2362	2473	2102	2312	155	7
21.1 °C	25	2004	1972	1880	1952	53	3
21.1 °C	10	1693	1695	1669	1686	12	1
21.1 °C	5	1509	1490	1482	1494	11	1
21.1 °C	1	1152	1124	1125	1134	13	1
21.1 °C	0.5	1018	990	996	1001	12	1
21.1 °C	0.1	738	706	724	723	13	2
37.8 °C	25	862	865	834	854	14	2
37.8 °C	10	688	689	671	683	8	1
37.8 °C	5	578	580	565	574	6	1
37.8 °C	1	371	379	367	373	5	1
37.8 °C	0.5	304	311	300	305	4	1
37.8 °C	0.1	181	189	180	183	4	2
54.4 °C	25	291	227	259	259	26	10
54.4 °C	10	209	168	190	189	17	9
54.4 °C	5	165	132	145	147	14	9
54.4 °C	1	94	80	80	85	6	8
54.4 °C	0.5	74	66	64	68	4	6
54.4 °C	0.1	47	46	39	44	3	8

Dynamic Modulus (ksi) values for all replicates for 25% RAP mix

Temp °C	Frequency Hz	25% RAP					
		4	5	6	AVG	std	cv%
10 °C	25	5944	8014	7599	7185	894	12
10 °C	10	5978	7637	7236	6950	706	10
10 °C	5	5873	7610	7238	6907	747	11
10 °C	1	5522	7110	6805	6479	688	11
10 °C	0.5	5366	6931	6630	6309	678	11
10 °C	0.1	4982	6436	6122	5847	625	11
4.4 °C	25	4473	5294	5622	5130	483	9
4.4 °C	10	4373	5058	5450	4960	445	9
4.4 °C	5	4162	4829	5147	4713	410	9
4.4 °C	1	3690	4216	4668	4191	400	10
4.4 °C	0.5	3505	4001	4362	3956	351	9
4.4 °C	0.1	3033	3484	3805	3441	317	9
21.1 °C	25	2677	3179	2604	2820	256	9
21.1 °C	10	2286	2754	2285	2441	221	9
21.1 °C	5	2045	2496	2055	2199	210	10
21.1 °C	1	1561	1957	1586	1702	181	11
21.1 °C	0.5	1379	1749	1410	1513	168	11
21.1 °C	0.1	1010	1312	1044	1122	135	12
37.8 °C	25	1175	1275	1353	1268	73	6
37.8 °C	10	958	1033	1104	1032	60	6
37.8 °C	5	819	898	942	886	51	6
37.8 °C	1	552	608	619	593	29	5
37.8 °C	0.5	465	505	511	494	20	4
37.8 °C	0.1	294	323	314	310	12	4
54.4 °C	25	350	462	375	396	48	12
54.4 °C	10	260	347	280	295	37	13
54.4 °C	5	206	271	222	233	28	12
54.4 °C	1	117	159	129	135	18	13
54.4 °C	0.5	93	131	101	108	16	15
54.4 °C	0.1	58	84	63	68	11	17

Dynamic Modulus values (ksi) for all replicates for 25% RAP + OS mix

Temp °C	Frequency Hz	25% RAP+OS					
		4	5	6	avg	std	cv%
10 °C	25	6961	6195	8054	7070	763	11
10 °C	10	6762	6113	7920	6932	747	11
10 °C	5	6577	5947	7625	6716	692	10
10 °C	1	6207	5551	7158	6306	660	10
10 °C	0.5	6064	5404	6946	6138	632	10
10 °C	0.1	5672	4995	6505	5724	617	11
4.4 °C	25	4485	5095	5545	5042	434	9
4.4 °C	10	4173	4653	5056	4627	361	8
4.4 °C	5	3962	4418	4769	4383	330	8
4.4 °C	1	3486	3905	4164	3852	279	7
4.4 °C	0.5	3280	3693	3939	3637	272	7
4.4 °C	0.1	2798	3176	3362	3112	235	8
21.1 °C	25	2544	2794	2386	2575	168	7
21.1 °C	10	2188	2422	2093	2234	138	6
21.1 °C	5	1934	2200	1892	2009	136	7
21.1 °C	1	1495	1683	1423	1534	109	7
21.1 °C	0.5	1345	1493	1258	1365	97	7
21.1 °C	0.1	968	1089	930	996	68	7
37.8 °C	25	1429	1244	923	1199	209	17
37.8 °C	10	1155	1010	769	978	159	16
37.8 °C	5	980	858	657	832	133	16
37.8 °C	1	618	550	412	527	86	16
37.8 °C	0.5	499	452	332	428	70	16
37.8 °C	0.1	299	270	193	254	45	18
54.4 °C	25	321	376	257	318	49	15
54.4 °C	10	231	267	191	230	31	13
54.4 °C	5	180	205	152	179	22	12
54.4 °C	1	99	116	81	99	14	14
54.4 °C	0.5	77	94	63	78	13	16
54.4 °C	0.1	47	63	38	50	10	20

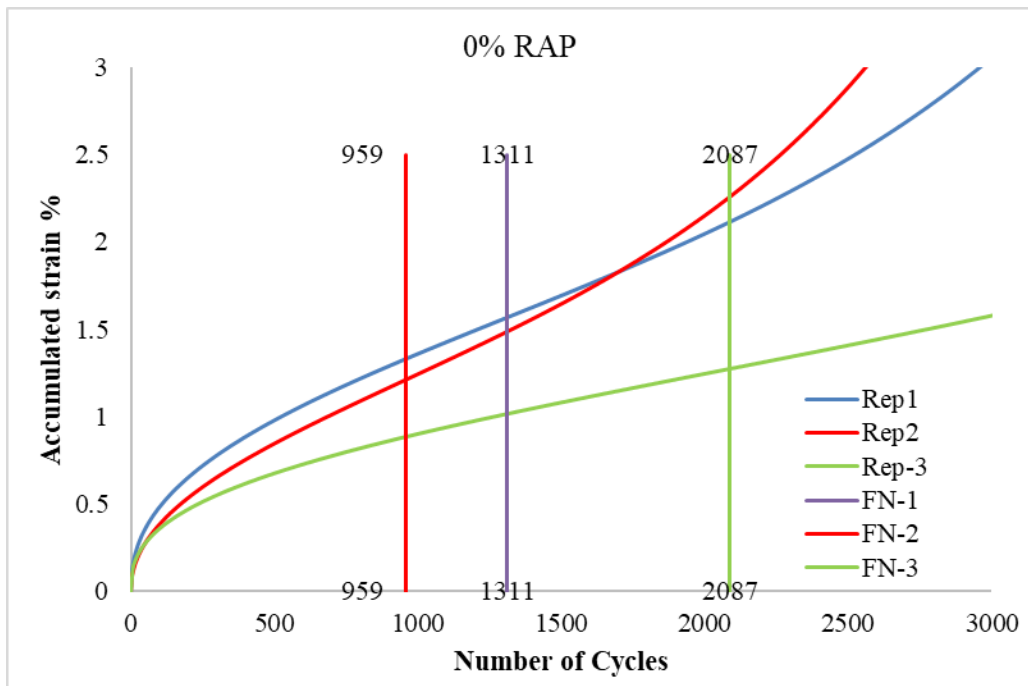
Hypothesis that the results of Dynamic modulus values when modified with Organosilane are equal to unmodified mixtures (student t analysis)

Temp, °F	Frequency Hz	0%RAP and 0%RAP+OS	15% RAP and 15% RAP+OS	25%RAP and 25%RAP+OS
14 °F	25	Accept	Accept	Accept
14	10	Accept	Reject	Accept
14	5	Accept	Reject	Accept
14	1	Accept	Reject	Accept
14	0.5	Accept	Reject	Accept
14	0.1	Accept	Reject	Accept
40 °F	25	Accept	Accept	Accept
40	10	Accept	Accept	Accept
40	5	Accept	Accept	Accept
40	1	Accept	Accept	Accept
40	0.5	Accept	Accept	Accept
40	0.1	Accept	Accept	Accept
70 °F	25	Accept	Accept	Accept
70	10	Accept	Accept	Accept
70	5	Accept	Accept	Accept
70	1	Accept	Accept	Accept
70	0.5	Accept	Accept	Accept
70	0.1	Reject	Accept	Accept
100 °F	25	Accept	Accept	Accept
100	10	Accept	Accept	Accept
100	5	Accept	Accept	Accept
100	1	Accept	Accept	Accept
100	0.5	Accept	Accept	Accept
100	0.1	Accept	Accept	Accept
130 °F	25	Accept	Accept	Accept
130	10	Accept	Accept	Accept
130	5	Accept	Reject	Accept
130	1	Accept	Reject	Accept
130	0.5	Accept	Reject	Accept
130	0.1	Accept	Accept	Accept

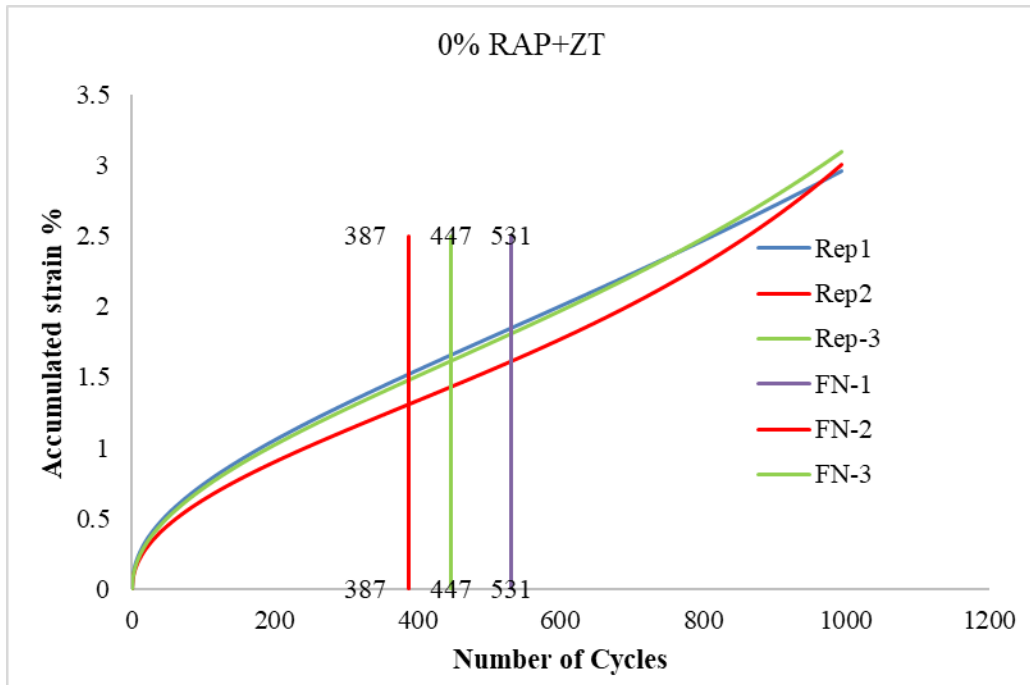
APPENDIX C
FLOW NUMBER VALUES

Flow number values for all six mixtures compared to specification limits

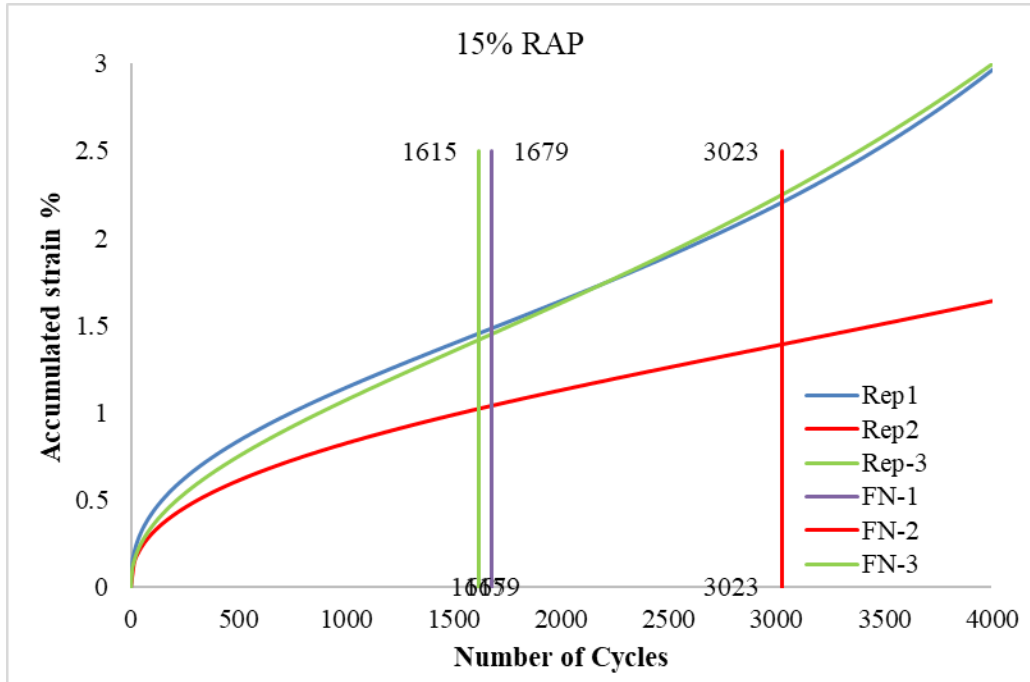
Mixture	FN	Range	Range as % Average	Limit of % Average
0% RAP	1452	1128	78	193
0%RAP+ OS	455	144	32	193
15% RAP	2106	1408	67	193
15%RAP+OS	754	188	25	193
25%RAP	5754	3056	53	193
25%RAP+OS	4090	4096	100	193



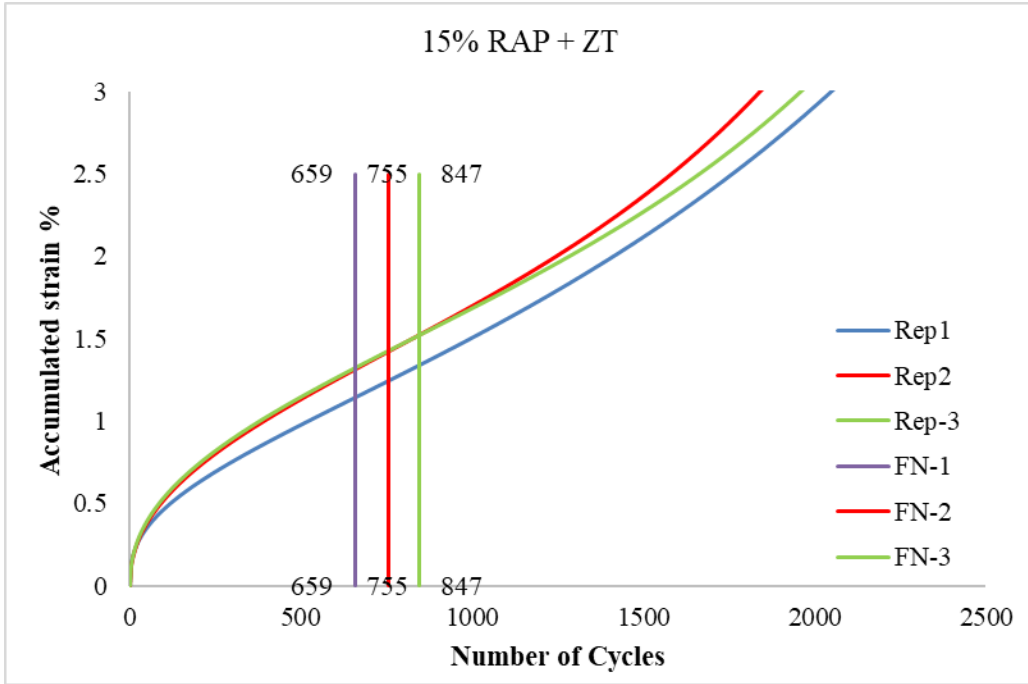
Plot for accumulated strain with number of cycles for all replicates of 0% RAP Mix



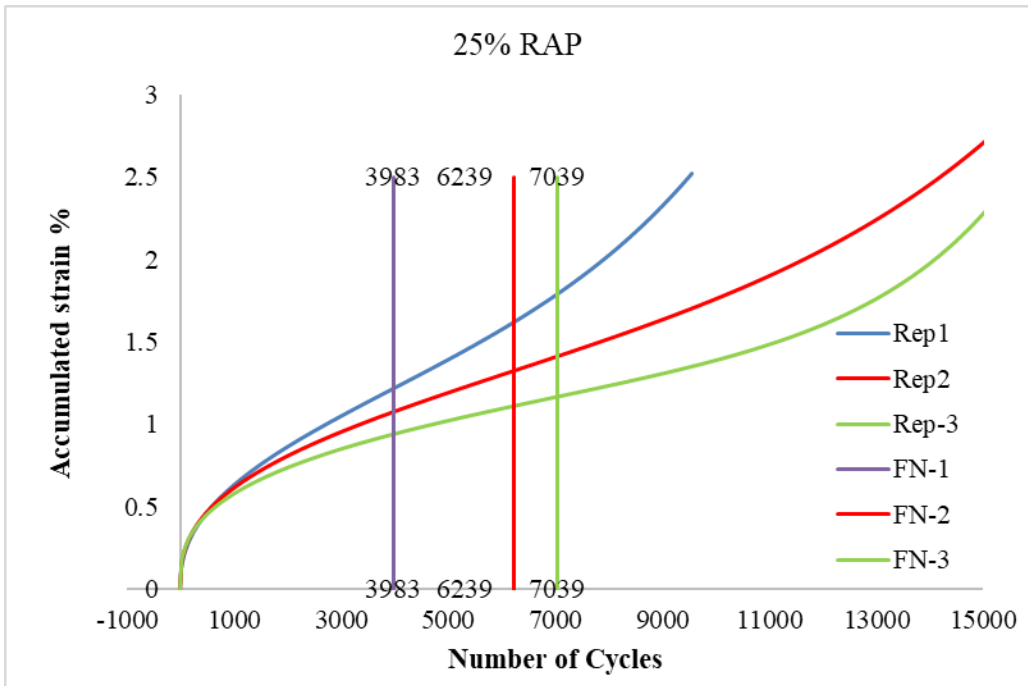
Plot for accumulated strain with number of cycles for all replicates of 0% RAP+OS Mix



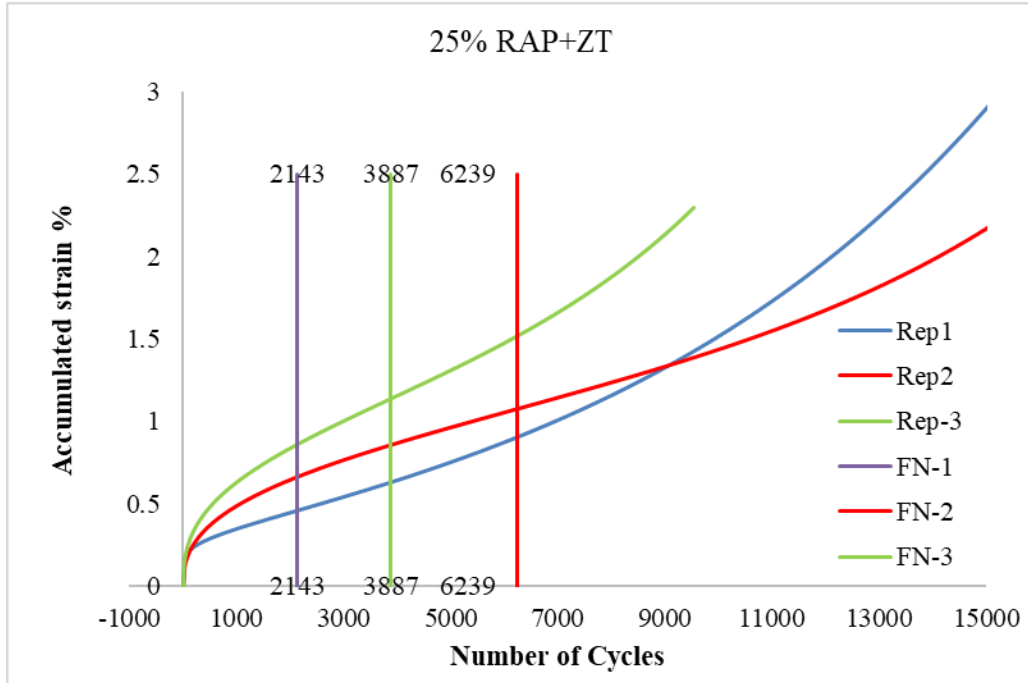
Plot for accumulated strain with number of cycles for all replicates of 15% RAP Mix



Plot for accumulated strain with number of cycles for all replicates of 15% RAP+OS Mix



Plot for accumulated strain with number of cycles for all replicates of 25% RAP Mix



Plot for accumulated strain with number of cycles for all replicates of 25% RAP+OS Mix

Hypothesis that the results of Flow number values when modified with Organosilane are equal to unmodified mixtures (student t analysis)

0% RAP and 0% RAP+OS	Accept
15% RAP and 15% RAP+OS	Accept
25% RAP and 25% RAP+OS	Accept

APPENDIX D
TENSILE STRENGTH RATIO CALCULATIONS

Tensile Strength Ratio calculation steps for 0% RAP mixture

Mix	Symbol	0% RAP						Average
Condition		Dry			Wet			
Sample identification		S1c-2	2-3T	2-3B	T-D2	C2-2	3-3B	
Diameter, mm (in.)	D	102.04	102.205	102.34	102.45	102.15	102.24	
Thickness, mm (in.)	t	63.9	64.4	64.9	66.5	62.4	65.0	
Dry Mass in air (gm)	A	1192.1	1215	1216.2	1223	1161.8	1216.3	
Mass in Water (gm)	C	674.4	693.3	693.8	692.6	658.8	695.7	
SSD mass (gm)	B	1194.3	1220.4	1220.8	1225	1163.3	1222.8	
Volume (B-C) cu.cm	E	519.9	527.1	527	532.4	504.5	527.1	
Bulk specific gravity	Gmb	2.293	2.305	2.308	2.297	2.303	2.308	
Gmm		2.474	2.474	2.474	2.474	2.474	2.474	
%Air voids [100(Gmm-Gmb)/Gmm]	Pa	7.3	6.8	6.7	7.1	6.9	6.7	
Vol. Air voids (Pa*E/100), cm ³	Va	38.05	35.99	35.41	38.06	34.90	35.47	
After saturation								
SSD (gm)	B'				1248.4	1183.2	1237.8	
Vol absorbed (B'-A) cu.cm	J'				25.4	21.4	21.5	
%Saturation (100J'/Va)					72.9	67.2	68.6	
Load N(lbf)	P	15985	15662	14990	13065	12839	13315	
Dry strength (2000*P/pi*t*D) kPa		1561	1516	1437				1505
Wet strength kPa					1222	1283	1276	1260
TSR		84						

Tensile Strength Ratio calculation steps for 0% RAP+OS mixture

Mix	Symbol	0% RAP+OS						Average
Condition		Dry			Wet			
Sample identification		5t	6t	6b	4t	4b	5b	
Diameter, mm (in.)	D	98	98	98	98	98	98	
Thickness, mm (in.)	t	60.0	61.0	64.0	62.0	64.0	60.0	
Dry Mass in air (gm)	A	1072.7	1125	1079.9	1089.6	1123.8	1064	
Mass in Water (gm)	C	613.6	637.3	612.1	617.7	638.8	608.1	
SSD mass (gm)	B	1074.2	1127	1081.8	1091.4	1126	1065.9	
Volume (B-C) cu.cm	E	460.6	489.7	469.7	473.7	487.2	457.8	
Bulk specific gravity	Gmb	2.329	2.297	2.299	2.300	2.307	2.324	
Gmm		2.458	2.458	2.458	2.458	2.458	2.458	
%Air voids [100(Gmm-Gmb)/Gmm]	Pa	5.3	6.5	6.5	6.4	6.2	5.4	
Vol. Air voids (Pa*E/100), cm ³	Va	24.19	32.01	30.36	30.41	30.00	24.93	
After saturation								
SSD (gm)	B'				1113	1145.9	1081.1	
Vol absorbed (B'-A) cu.cm	J'				23.4	22.1	17.1	
%Saturation (100J'/Va)					76.9414	73.6691	68.5983	
Load N(lbf)	P	17206	18387	16382	15958	15204	14368	
Dry strength (2000*P/pi*t*D) kPa		1863	1958	1663				1828
Wet strength kPa					1672	1543	1556	1590
TSR		87						

Tensile Strength Ratio calculation steps for 15% RAP mixture

Mix	Symbol	15% RAP						Average
Condition		Dry			Wet			
Sample identification		2-3T	3-3T	4-3T	3-3B	5c-1	1-3B	
Diameter, mm (in.)	D	102.355	102.155	102.185	102.385	102.175	102.32	
Thickness, mm (in.)	t	64.6	63.8	65.2	64.2	64.8	65.8	
Dry Mass in air (gm)	A	1198.5	1185.4	1205.4	1188.5	1200.6	1223.4	
Mass in Water (gm)	C	682.2	675.6	683.5	674	676.7	695.4	
SSD mass (gm)	B	1206.3	1192.7	1210.8	1193.7	1202.8	1228.3	
Volume (B-C) cu.cm	E	524.1	517.1	527.3	519.7	526.1	532.9	
Bulk specific gravity	Gmb	2.287	2.292	2.286	2.287	2.282	2.296	
Gmm		2.476	2.476	2.476	2.476	2.476	2.476	
%Air voids [100(Gmm-Gmb)/Gmm]	Pa	7.6	7.4	7.7	7.6	7.8	7.3	
Vol. Air voids (Pa*E/100), cm ³	Va	40.05	38.34	40.47	39.69	41.21	38.80	
After saturation								
SSD (gm)	B'				1210.4	1224.8	1244.8	
Vol absorbed (B'-A) cu.cm	J'				21.9	24.2	21.4	
%Saturation (100J'/Va)					65.2	69	65.8	
Load N(lbf)	P	15543	17197	17423	15531	13346	15808	
Dry strength (2000*P/pi*t*D) kPa		1496	1681	1665				1614
Wet strength kPa					1505	1283	1495	1428
TSR		88						

Tensile Strength Ratio calculation steps for 15% RAP+OS mixture

Mix	Symbol	15% RAP+OS						Average
Condition		Dry			Wet			
Sample identification		5t	6t	6b	4t	4b	5b	
Diameter, mm (in.)	D	98	98	98	98	98	98	
Thickness, mm (in.)	t	64.0	61.0	63.0	64.0	62.0	61.0	
Dry Mass in air (gm)	A	1126.5	1094.4	1114.4	1130.3	1074.5	1070.6	
Mass in Water (gm)	C	637.3	617.1	631.4	642.8	606.5	604.3	
SSD mass (gm)	B	1128.9	1096.5	1116.4	1134.1	1077	1072.5	
Volume (B-C) cu.cm	E	491.6	479.4	485	491.3	470.5	468.2	
Bulk specific gravity	Gmb	2.291	2.283	2.298	2.301	2.284	2.287	
Gmm		2.474	2.474	2.474	2.474	2.474	2.474	
%Air voids [100(Gmm-Gmb)/Gmm]	Pa	7.4	7.7	7.1	7.0	7.7	7.6	
Vol. Air voids (Pa*E/100), cm ³	Va	36.26	37.04	34.56	34.43	36.18	35.46	
After saturation								
SSD (gm)	B'				1154.9	1099.5	1098.2	
Vol absorbed (B'-A) cu.cm	J'				24.6	25	27.6	
%Saturation (100J'/Va)					71.4524	69.093	77.8353	
Load N(lbf)	P	16522	20041	20385	17796	17127	16144	
Dry strength (2000*P/pi*t*D) kPa		1677	2134	2102				1971
Wet strength kPa					1806	1795	1719	1773
TSR		90						

Tensile Strength Ratio calculation steps for 25% RAP mixture

Mix	Symbol	25% RAP						Average
Condition		Dry			Wet			
Sample identification		9b	10t	10b	8t	8b	9t	
Diameter, mm (in.)	D	100	100	100	100	100	100	
Thickness, mm (in.)	t	51.0	54.0	48.0	53.0	53.0	54.0	
Dry Mass in air (gm)	A	969.5	1027.9	901.7	984.6	997	1008.6	
Mass in Water (gm)	C	553.8	587.2	513.7	565.2	568.3	574	
SSD mass (gm)	B	970.6	1029.2	902.7	986.5	998.3	1010.2	
Volume (B-C) cu.cm	E	416.8	442	389	421.3	430	436.2	
Bulk specific gravity	Gmb	2.326	2.326	2.318	2.337	2.319	2.312	
Gmm		2.476	2.476	2.476	2.476	2.476	2.476	
%Air voids [100(Gmm-Gmb)/Gmm]	Pa	6.1	6.1	6.4	5.6	6.4	6.6	
Vol. Air voids (Pa*E/100), cm ³	Va	25.24	26.85	24.82	23.64	27.33	28.85	
After saturation								
SSD (gm)	B'				1001.2	1012.8	1026.8	
Vol absorbed (B'-A) cu.cm	J'				16.6	15.8	18.2	
%Saturation (100J'/Va)					70.2126	57.8026	63.0862	
Load N(lbf)	P	16495	16364	17124	15415	15030	17658	
Dry strength (2000*P/pi*t*D) kPa		2059	1929	2271				2086
Wet strength kPa					1852	1805	2082	1913
TSR		92						

Tensile Strength Ratio calculation steps for 25% RAP+OS mixture

Mix	Symbol	25% RAP+OS						Average
Condition		Dry			Wet			
Sample identification		8b	9t	10t	8t	9b	10b	
Diameter, mm (in.)	D	100	100	100	100	100	100	
Thickness, mm (in.)	t	51.0	55.0	48.0	51.0	50.0	53.0	
Dry Mass in air (gm)	A	953.9	1033	913.7	1010.7	941.3	952.4	
Mass in Water (gm)	C	545.2	588.7	523.7	576.1	538.5	545.5	
SSD mass (gm)	B	955.1	1034.4	914.8	1012.2	942.6	953.4	
Volume (B-C) cu.cm	E	409.9	445.7	391.1	436.1	404.1	407.9	
Bulk specific gravity	Gmb	2.327	2.318	2.336	2.318	2.329	2.335	
Gmm		2.474	2.474	2.474	2.474	2.474	2.474	
%Air voids [100(Gmm-Gmb)/Gmm]	Pa	5.9	6.3	5.6	6.3	5.8	5.6	
Vol. Air voids (Pa*E/100), cm ³	Va	24.33	28.16	21.78	27.57	23.62	22.94	
After saturation								
SSD (gm)	B'				1028.8	955.2	969.2	
Vol absorbed (B'-A) cu.cm	J'				18.1	13.9	16.8	
%Saturation (100J'/Va)					65.648	58.8409	73.2461	
Load N(lbf)	P	18378	20935	18347	17832	17902	19306	
Dry strength (2000*P/pi*t*D) kPa		2294	2423	2433				2384
Wet strength kPa					2226	2279	2319	2275
TSR		95						